JOURNAL OF PETROLOGY | VOLUME 52 | NUMBER 6 | PAGES 1185–1206 | 2011 | doi:10.1093/petrology/egr024

Geochemical Composition of K-rich Lavas from the Lena Trough (Arctic Ocean)

F. NAURET[1,2]*, J. E. SNOW[2,3], E. HELLEBRAND[2,4] AND D. WEIS[1]

[1]PACIFIC CENTRE FOR ISOTOPIC AND GEOCHEMICAL RESEARCH, EARTH AND OCEAN SCIENCES, UNIVERSITY OF BRITISH COLUMBIA, 6339 STORES ROAD, VANCOUVER, BC, V6T 1Z4, CANADA

[2]MAX-PLANCK INSTITUT FÜR CHEMIE, POSTFACH 3060, 55122 MAINZ, GERMANY

[3]DEPARTMENT OF GEOSCIENCES, UNIVERSITY OF HOUSTON, HOUSTON, TX 77204-5007, USA

[4]UNIVERSITY OF HAWAII, DEPARTMENT OF GEOLOGY AND GEOPHYSICS, HONOLULU, HI 96822, USA

RECEIVED NOVEMBER 4, 2009; ACCEPTED APRIL 24, 2011
ADVANCE ACCESS PUBLICATION JUNE 9, 2011

Mid-ocean ridge basalts (MORB) from the Arctic Ocean have been significantly less studied than those from other oceans. The Arctic ridges (Gakkel Ridge and Lena Trough) are ultraslow-spreading ridges with low melt productivity and are thus the best locations to investigate mantle heterogeneity. We report the major and trace element and Sr–Nd–Pb–Hf isotope compositions of basalts generated along the Lena Trough and the westernmost part of the Gakkel Ridge in the Arctic Ocean. Basalts from the northern Lena Trough and westernmost Gakkel Ridge (NLT–WGR) have compositions close to normal MORB. The geochemical composition of the NLT–WGR lavas confirms a binary mixing model involving melts from a depleted MORB mantle source and a Spitsbergen amphibole-bearing subcontinental lithospheric mantle (SCLM) source. In contrast, in the central part of the Lena Trough (CLT), the basalts are alkalic with relatively high Mg-number (60–65), high SiO_2 (51·0–51·6 wt %), Al_2O_3 (18·1–18·4 wt %), Na_2O (4·0–4·2 wt %), K_2O (1·0–1·6 wt %), K_2O/TiO_2 (0·6–0·9) and $(La/Sm)_{PM}$ (1·4–1·8), and low FeO (6·5–6·8 wt %) contents. These basalts display isotope variations with $^{87}Sr/^{86}Sr$ ranging from 0·70361 to 0·70390, $^{143}Nd/^{144}Nd$ from 0·51283 to 0·51290 (ε_{Nd} + 3·7 to +5·2), $^{176}Hf/^{177}Hf$ from 0·28313 to 0·28322 (ε_{Hf} + 11·6 to +14·9) and $^{206}Pb/^{204}Pb$ from 17·752 to 17·884, $^{207}Pb/^{204}Pb$ from 15·410 to 15·423 and $^{208}Pb/^{204}Pb$ from 37·544 to 37·670. These isotope compositions clearly distinguish the CLT lavas from those generated along the Gakkel Ridge. For the CLT lavas, involvement of a phlogopite- or amphibole- and (possibly garnet)-bearing SCLM source component is proposed. Owing to SCLM contamination along the entire length of the Lena Trough, we classify the Lena Trough as an ocean–continent transition boundary. Magmatism similar to that observed in the Lena Trough would be expected to occur wherever ocean spreading initiates.

KEY WORDS: *major and trace elements; Sr–Nd–Pb–Hf isotopes; ultraslow-spreading ridge; low-degree melt; Arctic Ocean; MORB; ocean–continent transition boundary*

INTRODUCTION

The distribution of incompatible-element-enriched components in the mantle has been under discussion for over 30 years (e.g. Wood *et al.*, 1979). Many researchers have argued for a relatively homogeneous upper mantle that is in chemical equilibrium over a large area (Hofmann & Hart, 1978). However, basalts from ocean islands, and in some cases from mid-ocean ridges, show trends that indicate mixing between melts of distinct mantle sources that are sampled over a wide area (e.g. le Roex *et al.*, 1981). The mixing generally occurs between an early melt fraction and melts derived from upper mantle peridotite at a relatively high level in the mantle (le Roex *et al.*, 1992). Studies of peridotites from the SW Indian Ridge have documented clinopyroxene compositions indicative of disequilibrium between the peridotites and melts sampled nearby (Salters & Dick, 2002; Snow *et al.*, 1994), which provides some evidence in favor of such a mixing model. The data

*Corresponding author. Present address: Laboratoire Magmas et Volcans, Université Blaise Pascal, 5 rue Kessler, BP 10448, 63000 Clermont-Ferrand, France.
E-mail: F.Nauret@opgc.univ-bpclermont.fr

seem to suggest that a low-degree melt component derived from hydrous mantle veins is the major source of enriched material at mid-ocean ridges. As most of the heat-producing elements (i.e. U, Th, K) in the mantle are strongly lithophile, such enriched regions constitute an important source for the radiogenic internal heating of the mantle; they represent a major repository of water, and are potentially derived from deep recycling of crustal materials. However, in all preceding studies, melts derived from a supposed veined mantle source form only a small part of a basaltic magma series that could otherwise be generated by the partial melting of peridotite. In the case of the peridotite data, this inference is based on the absence of a large ion lithophile element (LILE)-enriched component in the peridotites that has been observed in associated basalts (Salters & Dick, 2002; Snow *et al.*, 1994). Furthermore, although pyroxenite veins in peridotite massifs worldwide are commonplace, the vein assemblages generally cross-cut features related to or post-dating melting. The existence of mantle veins that clearly pre-date melting has never been documented in a mid-ocean ridge sample. Even though such veins would not be expected to survive partial melting, it is nevertheless conceptually difficult to argue in favor of their existence, particularly in mantle regions that have undergone little or no partial melting. Thus, the evidence for mantle veins as a widespread phenomenon is tenuous at best, and the vast majority of mid-ocean ridge basalts are likely to be generated by peridotite partial melting alone.

The natural place to look for melt veins or mineralogical evidence for mantle heterogeneity is at ultraslow-spreading mid-ocean ridges because here the degree of melting in the mantle is reduced by the thick overlying lithosphere, resulting in a relatively thin crust (Reid & Jackson, 1981; Bown & White, 1994; Hellebrand & Snow, 2003). Thus there may be a higher proportion of any vein-derived material in the source of the basalts generated at such localities. For example, a recent study of the South West Indian Ridge (SWIR) between 9 and 25°E concluded that certain high K/Ti mid-ocean ridge basalt (MORB) samples result from heterogeneities in the underlying mantle and also from the local thermal structure of the lithosphere (Standish *et al.*, 2008). To examine such mantle heterogeneities, the Arctic Ocean spreading ridges—the Gakkel Ridge and the Lena Trough—were recently extensively sampled and studied. Owing to its obliquity, the Lena Trough has a slower effective spreading rate (~7·5 mm a^{-1}, effective full rate) than the Gakkel Ridge (6–13 mm a^{-1}, full spreading rate; Jokat *et al.*, 2003).

A DUPAL-like geochemical anomaly has been observed in the basalts of the Arctic Ocean (Mühe *et al.*, 1993, 1997), especially around the western Gakkel Ridge (Goldstein *et al.*, 2008). The origin of this northern DUPAL anomaly has been attributed to the presence of a fragment of subcontinental lithospheric mantle (SCLM) from Spitsbergen, in the western part of the Gakkel Ridge mantle (Goldstein *et al.*, 2008). This recycled SCLM component is thought to include hydrous veins, and could thus be a source of mantle heterogeneity.

Based on osmium isotopes measured in mantle peridotites, the presence of ancient refractory mantle zones has also been inferred along the Gakkel Ridge (Liu *et al.*, 2008), confirming the existence of mineralogical heterogeneity in the mantle. Similar geochemical features (i.e. mantle heterogeneity) are expected along the Lena Trough, where a strong influence of an SCLM component is anticipated owing to the proximity of Spitsbergen and Greenland; enriched SCLM is often invoked for the North Atlantic–Arctic Ocean zones (Blichert-Toft *et al.*, 2005; Debaille *et al.*, 2006; Goldstein *et al.*, 2008). Nevertheless, there is some ambiguity about the role of an SCLM component in the Lena Trough mantle. Preliminary osmium isotope data for Lena Trough peridotites fall within the range reported for abyssal peridotites globally, which suggests that the contribution of the SCLM component is limited, and that the Lena Trough peridotites do not represent mantle from an ocean–continent transitional boundary (Lassiter & Snow, 2009).

To evaluate the potential contribution of Greenland–Spitsbergen subcontinental lithospheric mantle in MORB petrogenesis, and thus the heterogeneity of the underlying mantle, we have analyzed the chemical compositions of basalts collected during the PFS *Polarstern* cruises ARK XV/2 (Jokat, 2000), ARK XVII-2 (Snow *et al.*, 2002) ARK-XX-2 (Snow *et al.*, 2007), and USCGC *Healy* Cruise HLY0102 (Michael *et al.*, 2001) along the Lena Trough (Fig. 1). We present here major element, trace element and Sr–Nd–Pb–Hf isotope data for these basalts.

SAMPLE LOCATIONS AND ANALYTICAL METHODS

Sample locations and mineralogy

Dredge locations from the ARK-XX-2, ARK XVII-2 and HLY0102 cruises containing volcanic rocks are shown in Fig. 1 and reported in Table 1. Glassy pillow basalt samples were collected in three areas: Central Lena Trough (CLT) with dredges PS66-261, 262 and PS55-90; Northern Lena Trough (NLT) with dredges PS66-219, 217, HLY0102-D8 and D11; and westernmost Gakkel Ridge (GR) with dredges PS59-216, 218, 221, 223 and PS66-214 (Table 1). Basalt types, discriminated based on their mineralogy, are either plagioclase or olivine phyric, plagioclase–olivine phyric, or aphyric. The groundmass is mainly composed of plagioclase, olivine and clinopyroxene microlites in a glassy matrix. A major difference between these basalt types is the amount of vesicles. Westernmost Gakkel Ridge MORB and Northern Lena Trough basalts display only a

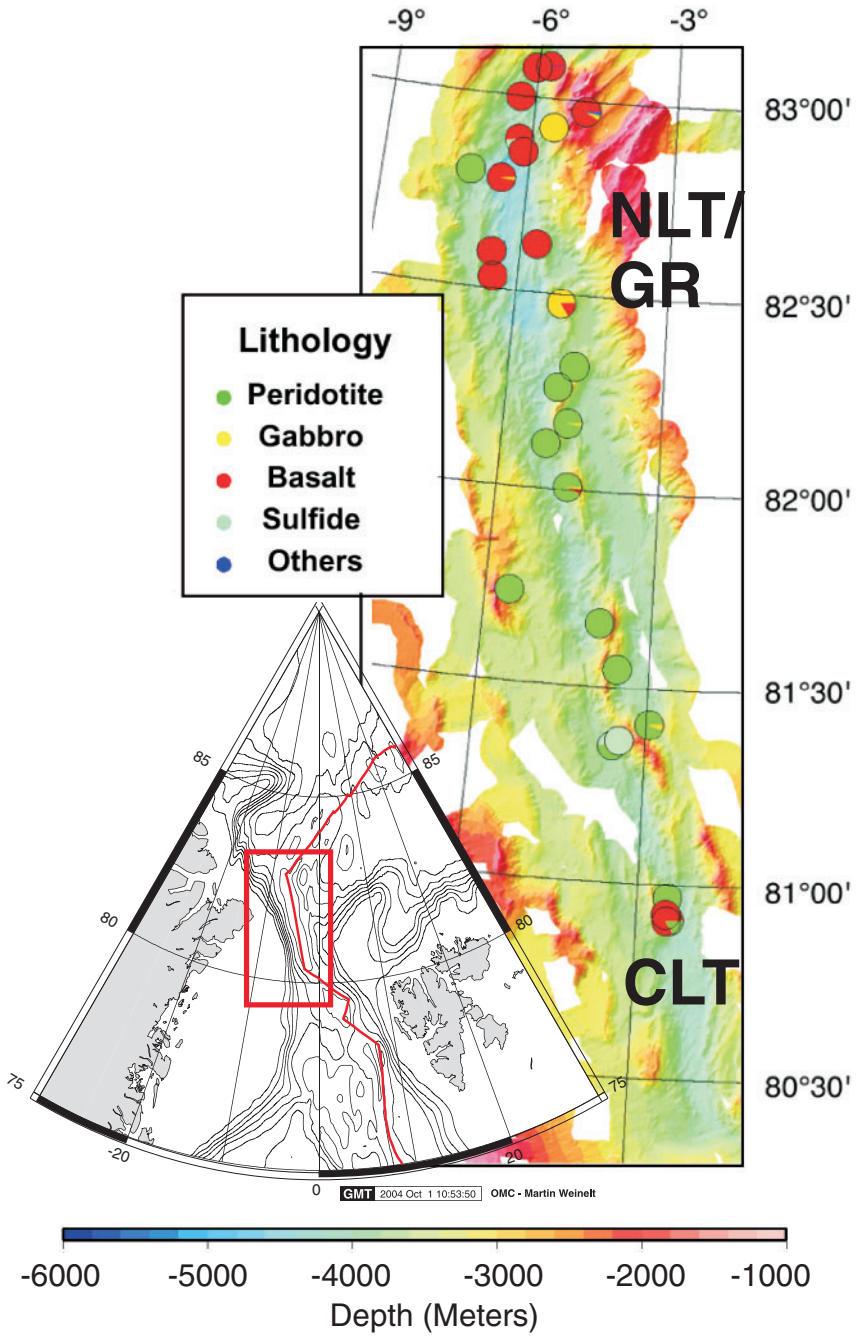

Fig. 1. Bathymetric map of the Lena Trough. Geographical coordinates of the sample locations are given in Table 1.

low percentage of vesicles (<1 to 5%). In contrast, basalts collected in the southern part of the Lena Trough are highly vesicular (up to 25%) despite water depths of over 3500 m (Snow *et al.*, 2007).

Analytical methods

Major element compositions were analyzed using a JEOL Super-probe 8200 electron microprobe and trace element compositions by laser ablation inductively coupled plasma mass spectrometry (LA-ICP-MS), both at the Max Planck Institut für Chemie (Mainz). All analyses were carried out on hand-picked glass chips from the rims of pillows mounted in an epoxy ring. Major and trace element compositions were measured on the same chip. Major element analyses were performed using a 20 kV accelerating voltage and a 2 μm diameter beam. VG-2 was used as a standard

Table 1: Sample location, Major and trace element compositions of Central (CLT) and Northern Lena Trough/ Westernmost Gakkel Ridge (NLT/WGR) lavas. Samples were collected during several cruises: PS55 = ARK XV/2 (1999), PS59 = ARK XVII/2 (2001), PS66 = ARK XX/2 (2004) PFS Polarstern, Alfred Wegener Institute for Polar and Marine Research, Bremerhaven, Germany, and HLY 0102 = USCGC Healy, Cruise 1 Leg 2 (2001) (Jokat 2000). Analytical procedures are detailed in supplementary information.

Cruise:	PS66										
Sample:	262-92	262-83	262-35	262-34	262-21	261-71	261-5	261-47	261-1	261-17	261-12
Lat. (N):	80·90	80·90	80·90	80·90	80·90	80·92	80·92	80·9243	80·9243	80·9243	80·9243
Long. (W):	−2·50	−2·50	−2·50	−2·50	−2·50	−2·52	−2·52	−2·5253	−2·5253	−2·5253	−2·5253
Central Lena Trough (ARK XX/2)											
SiO_2	51·3	51·1	51·3	51·4	51·2	51·3	51·4	51·1	51·2	51·6	51·5
TiO_2	1·69	1·68	2·21	2·22	1·68	1·59	1·56	1·59	1·55	1·60	1·58
Al_2O_3	18·34	18·33	18·16	18·31	18·44	18·21	18·25	18·10	18·18	18·29	18·15
CaO	9·60	9·52	8·63	8·68	9·56	9·76	9·74	9·69	9·72	9·84	9·72
FeO	6·54	6·52	6·69	6·79	6·57	6·55	6·60	6·55	6·66	6·52	6·63
MgO	6·14	6·10	5·22	5·05	6·14	6·35	6·39	6·48	6·44	6·24	6·46
MnO	0·11	0·15	0·15	0·15	0·12	0·12	0·13	0·13	0·12	0·13	0·13
Na_2O	4·13	4·04	4·00	4·06	4·10	4·20	4·12	4·14	4·11	4·15	4·10
K_2O	1·25	1·26	1·94	1·98	1·24	1·01	1·01	1·01	1·01	1·003	1·008
P_2O_5	0·21	0·20	0·28	0·28	0·22	0·20	0·20	0·19	0·17	0·184	0·183
S	0·05	0·05	0·04	0·05	0·06	0·05	0·06	0·04	0·06	0·05	0·06
Cl	0·02	0·02	0·04	0·03	0·02	0·02	0·02	0·02	0·02	0·02	0·02
Total	99·41	98·94	98·69	99·01	99·31	99·37	99·41	99·02	99·26	99·62	99·49
Cs	0·44	0·45	0·76	0·74	0·43	0·35	0·35	0·35	0·35	0·34	0·34
Rb	32·0	33·2	53·1	52·3	32·0	26·3	26·7	26·2	26·0	25·8	25·7
Ba	297	300	488	486	298	252	247	255	241	247	239
Th	0·84	0·78	1·27	1·30	0·77	0·69	0·65	0·69	0·64	0·67	0·64
U	0·25	0·25	0·40	0·42	0·25	0·21	0·20	0·21	0·20	0·21	0·20
Nb	17·2	17·7	28·5	28·7	17·6	15·5	14·9	15·3	15·1	15·2	14·5
Ta	1·20	1·22	1·92	1·99	1·24	1·05	1·02	1·06	1·00	1·02	0·99
La	9·1	9·2	13·3	13·3	9·1	8·4	8·1	8·4	7·9	8·2	7·8
Ce	22·6	23·1	32·3	32·4	22·9	21·3	20·71	21·5	20·4	20·9	20·1
Pr	3·28	3·34	4·60	4·58	3·30	3·10	3·01	3·16	2·31	3·01	2·92
Sr	354	354	444	444	354	322	324	318	324	318	317
Pb	1·05	1·09	1·39	1·39	1·05	1·03	0·99	1·03	0·98	1·03	0·96
Nd	15·0	15·3	20·4	20·6	15·1	14·4	13·9	14·5	13·9	14·0	13·5
Zr	134	137	176	182	138	130	123	127	125	127	123
Hf	3·14	3·21	4·03	4·25	3·25	3·11	2·95	3·04	2·92	3·04	2·88
Sm	3·67	3·75	4·71	4·78	3·70	3·65	3·53	3·68	3·48	3·54	3·44
Eu	1·36	1·37	1·68	1·68	1·34	1·34	1·31	1·37	1·30	1·31	1·28
Gd	3·97	4·09	4·79	4·87	4·04	4·18	4·02	4·13	3·93	4·05	3·92
Tb	0·62	0·64	0·71	0·72	0·63	0·67	0·63	0·67	0·64	0·64	0·63
Dy	3·77	3·84	4·15	4·23	3·86	4·16	3·93	4·14	3·96	4·03	3·82
Ho	0·74	0·76	0·79	0·82	0·76	0·83	0·79	0·83	0·79	0·82	0·77
Er	2·15	2·20	2·23	2·29	2·19	2·44	2·28	2·42	2·27	2·34	2·20
Tm	0·29	0·30	0·30	0·31	0·30	0·33	0·31	0·33	0·31	0·32	0·30
Y	20·9	21·5	22·1	22·9	21·7	23·5	21·8	22·7	22·0	23·0	21·8
Yb	1·97	2·00	2·05	2·04	2·02	2·25	2·11	2·22	2·10	2·18	2·02
Lu	0·29	0·29	0·30	0·30	0·30	0·33	0·31	0·32	0·30	0·32	0·30
Ni	80·7	80·8	58·8	57·4	81·1	89·7	95·5	95·1	95·6	89·8	91·4
Sc	29·4	29·2	27·1	28·1	29·9	31·1	30·8	29·9	30·8	31·4	30·8

(continued)

Table 1: Continued

Cruise:	PS55						
Sample:	90-1	90-3	90-4	90-7	90-9	90-10	90-27
Lat. (N):	80·908	80·908	80·908	80·908	80·908	80·908	80·908
Long. (W):	−2·508	−2·508	−2·508	−2·508	−2·508	−2·508	−2·508
Central Lena Trough (ARK XV/2)							
SiO_2	51·5	51·4	51·5	51·6	51·8	51·5	51·4
TiO_2	2·00	2·00	2·01	2·02	2·02	2·03	2·01
Al_2O_3	18·30	18·31	18·35	18·36	18·36	18·34	18·32
CaO	9·01	9·00	9·10	8·97	9·10	8·94	8·99
FeO	6·64	6·71	6·65	6·59	6·70	6·63	6·67
MgO	5·70	5·71	5·73	5·66	5·62	5·68	5·69
MnO	0·12	0·15	0·13	0·13	0·13	0·13	0·14
Na_2O	3·87	3·84	3·88	3·95	3·89	3·90	3·89
K_2O	1·54	1·55	1·55	1·56	1·51	1·55	1·55
P_2O_5	0·27	0·27	0·26	0·27	0·28	0·26	0·27
S	0·05	0·04	0·04	0·04	0·05	0·04	0·05
Cl	0·02	0·03	0·03	0·03	0·03	0·03	0·03
Total	99·01	99·03	99·18	99·14	99·44	98·99	99·00
Cs	0·58	0·59	0·59	0·59	0·59	0·58	0·59
Rb	41·7	42·3	42·0	43·0	41·8	41·9	41·9
Ba	385	389	386	389	389	384	384
Th	1·02	1·02	1·13	1·01	1·02	1·00	1·00
U	0·32	0·32	0·32	0·32	0·33	0·32	0·32
Nb	22·6	22·9	22·4	22·7	22·8	22·4	22·4
Ta	1·59	1·59	1·59	1·59	1·59	1·57	1·58
La	11·2	11·3	11·3	11·2	11·2	11·0	11·0
Ce	27·8	27·9	28·0	28·0	28·4	27·7	27·8
Pr	4·00	4·03	4·02	4·02	4·06	3·96	3·97
Sr	401	402	402	400	402	397	395
Pb	1·28	1·32	1·28	1·24	1·28	1·28	1·29
Nd	18·3	18·2	18·3	18·2	18·4	17·9	18·0
Zr	166	167	166	164	164	162	161
Hf	3·90	3·88	3·89	3·84	3·87	3·82	3·80
Sm	4·38	4·32	4·39	4·33	4·40	4·27	4·24
Eu	1·57	1·54	1·57	1·56	1·59	1·54	1·54
Gd	4·62	4·60	4·66	4·59	4·66	4·48	4·49
Tb	0·70	0·70	0·71	0·69	0·71	0·68	0·69
Dy	4·22	4·15	4·26	4·18	4·20	4·09	4·07
Ho	0·82	0·82	0·82	0·82	0·83	0·81	0·80
Er	2·35	2·32	2·35	2·33	2·37	2·28	2·26
Tm	0·32	0·31	0·32	0·32	0·32	0·31	0·31
Y	23·0	23·1	23·1	22·7	22·8	22·5	22·3
Yb	2·13	2·11	2·15	2·13	2·12	2·12	2·07
Lu	0·32	0·31	0·31	0·31	0·31	0·30	0·30
Ni	68·1	68·6	67·6	68·2	65·3	65·4	67·5
Sc	29·0	29·0	29·4	28·6	28·9	28·5	28·5

(continued)

Table 1: Continued

Cruise:	PS66											
Sample:	217-5	217-6	217-7	217-4	217-8	217-9	217-1	217-3	219-1	219-2	VG2	ATHO
Lat. (N):	82·85	82·85	82·85	82·85	82·85	82·85	82·85	82·85	82·78	82·78		
Long. (W):	−6·14	−6·14	−6·14	−6·14	−6·14	−6·14	−6·14	−6·14	−6·54	−6·54		
NLT/WGR												
SiO_2	52·2	50·6	50·5	50·7	50·6	50·7	50·6	50·4	50·5	49·4	50·9	
TiO_2	1·79	1·75	1·74	1·76	1·72	1·78	1·74	1·75	1·77	1·91	1·89	
Al_2O_3	16·39	16·01	15·79	15·97	15·84	15·96	16·07	15·97	15·95	17·45	14·06	
CaO	10·99	10·66	10·64	10·67	10·65	10·75	10·65	10·65	10·63	10·29	11·02	
FeO	10·02	9·62	9·70	9·60	9·72	9·65	9·53	9·55	9·65	9·76	11·88	
MgO	7·33	7·12	7·11	7·14	7·50	6·88	7·06	7·11	7·23	6·63	6·72	
MnO	0·170	0·187	0·158	0·158	0·195	0·168	0·178	0·157	0·178	0·165	0·21	
Na_2O	1·44	3·40	3·32	3·38	3·38	3·42	3·39	3·35	3·32	3·54	2·89	
K_2O	0·35	0·36	0·36	0·36	0·366	0·367	0·367	0·369	0·359	0·663	0·19	
P_2O_5	0·159	0·174	0·161	0·159	0·164	0·153	0·166	0·168	0·159	0·121	0·22	
S	0·11	0·10	0·10	0·10	0·10	0·11	0·11	0·10	0·12	0·09	0·13	
Cl	0·01	0·01	0·01	0·01	0·01	0·01	0·01	0·01	0·01	0·01	0·03	
Total	100·95	100·05	99·60	99·99	100·28	99·95	99·90	99·56	99·90	100·04	100·14	
Cs	0·11	0·12	0·12	0·12	0·12	0·12	0·12	0·11	0·12	0·32		0·86 ± 0·02
Rb	7·73	8·07	8·08	7·98	8·17	8·03	8·41	8·35	8·34	17·65		59 ± 1·0
Ba	79·3	83·1	85·8	81·5	85·3	84·1	82·2	86·2	82·3	161		534 ± 7
Th	6·02	0·48	0·36	3·42	0·35	0·35	0·36	0·35	0·34	0·68		7·3 ± 0·1
U	0·10	0·10	0·10	0·10	0·10	0·10	0·10	0·10	0·10	0·17		2·24 ± 0·04
Nb	4·86	5·31	5·54	5·18	5·47	5·42	5·23	5·52	5·50	8·34		58 ± 1
Ta	0·27	0·35	0·37	0·35	0·36	0·35	0·35	0·37	0·37	0·59		3·6 ± 0·1
La	4·54	4·84	5·06	4·86	4·99	5·07	4·75	5·05	4·80	5·92		53 ± 1
Ce	12·57	14·12	14·74	14·13	14·60	14·86	13·50	14·84	14·11	16·25		118 ± 1
Pr	2·13	2·38	2·46	2·38	2·45	2·50	2·32	2·49	2·36	2·56		14·51 ± 0·11
Sr	176	189	193	184	190	191	181	191	190	272		96 ± 1
Pb	1·30	0·61	0·62	0·62	0·63	0·63	0·59	0·64	0·66	1·14		5·7 ± 0·5
Nd	11·12	12·49	12·88	12·53	12·79	13·10	12·15	13·01	12·35	12·63		58 ± 1
Zr	108	116	122	114	119	123	106	121	118	101		503 ± 9
Hf	2·84	3·04	3·24	3·05	3·20	3·29	2·84	3·26	3·19	2·75		13·5 ± 0·30
Sm	3·95	4·07	4·12	3·98	4·16	4·25	3·93	4·18	3·96	3·63		13·4 ± 0·20
Eu	1·29	1·48	1·52	1·48	1·53	1·55	1·43	1·53	1·47	1·42		2·63 ± 0·04
Gd	4·66	5·40	5·62	5·38	5·57	5·70	5·11	5·64	5·36	4·44		14·8 ± 0·2
Tb	0·80	0·94	0·97	0·93	0·96	0·98	0·90	0·97	0·93	0·74		2·5 ± 0·04
Dy	5·40	6·03	6·32	6·04	6·26	6·43	5·73	6·33	6·10	4·64		16·0 ± 0·20
Ho	1·17	1·26	1·32	1·24	1·31	1·34	1·19	1·32	1·26	0·94		3·3 ± 0·1
Er	3·39	3·72	3·86	3·75	3·91	3·96	3·38	3·88	3·73	2·72		10·1 ± 0·2
Tm	0·47	0·51	0·53	0·52	0·54	0·55	0·49	0·53	0·52	0·37		1·5 ± 0·0.1
Y	31·05	35·51	37·26	34·78	36·22	37·59	32·10	36·50	35·62	26·98		96 ± 2
Yb	3·14	3·52	3·64	3·59	3·61	3·75	3·44	3·66	3·62	2·52		10·2 ± 0·1
Lu	0·45	0·52	0·55	0·51	0·54	0·55	0·49	0·54	0·53	0·37		1·5 ± 0·1
Ni	103	106	106	99	119	114	99	109	112	89		3·9 ± 1·0
Sc	37·1	38·6	40·4	38·1	40·1	41·1	36·5	40·2	40·4	35·8		6·0 ± 0·1

(continued)

Table 1: Continued

Cruise:	HLY-0102											
Sample:	D8-16	D8-11	D8-13	D8-16	D8-17	D8-1	D8-21	D8-22	D8-8	D11-5	D11-9	D11-22
Lat. (N):	82·89	82·89	82·89	82·89	82·89	82·89	82·89	82·89	82·89	83	83	83
Long. (W):	−6·26	−6·26	−6·26	−6·26	−6·26	−6·26	−6·26	−6·26	−6·26	−6·32	−6·32	−6·32
NLT/WGR												
SiO_2	50·7	50·4	50·8	50·7	49·7	50·6	50·8	50·6	50·7	51·0	50·8	50·6
TiO_2	1·50	1·58	1·50	1·52	1·20	1·51	1·55	1·51	1·57	1·56	1·55	1·57
Al_2O_3	15·65	15·42	15·69	15·70	16·66	15·66	15·55	15·67	15·44	16·03	16·06	15·91
FeO	9·33	9·52	9·40	9·34	8·94	9·42	9·51	9·41	9·48	9·24	9·12	9·18
MnO	0·18	0·18	0·17	0·17	0·17	0·16	0·16	0·16	0·17	0·16	0·16	0·16
MgO	7·66	7·61	7·80	7·74	8·24	7·73	7·60	7·73	7·57	7·48	7·47	7·46
CaO	11·03	10·97	10·97	10·94	11·85	10·98	10·95	11·00	11·00	10·88	10·86	10·86
Na_2O	3·17	3·18	3·01	3·18	2·94	3·19	3·14	3·20	3·17	3·14	3·23	3·26
K_2O	0·20	0·21	0·20	0·22	0·07	0·20	0·20	0·20	0·21	0·32	0·31	0·32
P_2O_5	0·15	0·15	0·14	0·13	0·08	0·16	0·14	0·17	0·15	0·16	0·15	0·15
S	0·10	0·11	0·10	0·10	0·11	0·10	0·10	0·11	0·11	0·11	0·10	0·10
Cl	0·01	0·01	0·01	0·01	0·01	0·01	0·01	0·01	0·01	0·01	0·01	0·01
Total	99·73	99·33	99·74	99·75	99·94	99·71	99·70	99·80	99·58	100·11	99·77	99·60
Cs	0·05	0·05	0·05	0·05	0·01	0·05	0·05	0·05	0·05	0·09	0·09	0·09
Rb	3·84	3·52	3·71	3·70	0·62	3·70	3·51	3·72	3·53	6·89	6·85	6·80
Ba	46·9	43·4	44·9	45·7	7·6	44·7	43·8	45·4	43·4	73·6	72·2	71·9
Th	0·24	0·26	0·25	0·24	0·06	0·25	0·25	0·25	0·26	0·30	0·30	0·30
U	0·07	0·07	0·06	0·06	0·02	0·06	0·07	0·06	0·07	0·08	0·08	0·08
Nb	3·22	3·01	3·08	3·17	0·84	3·09	3·09	3·14	3·06	4·99	4·90	4·86
Ta	0·20	0·20	0·21	0·19	0·05	0·20	0·19	0·20	0·20	0·33	0·34	0·34
La	3·84	3·94	3·77	3·76	1·93	3·74	3·93	3·82	3·94	4·49	4·41	4·44
Ce	11·5	11·5	11·0	11·1	6·7	11·0	11·6	11·1	11·5	12·7	12·5	12·4
Pr	1·94	1·97	1·86	1·90	1·24	1·93	1·98	1·90	1·95	2·07	2·06	2·04
Sr	154	147	147	150	126	148	147	149	148	175	173	172
Pb	0·53	0·54	0·53	0·54	0·32	0·53	0·55	0·52	0·55	0·55	0·56	0·56
Nd	10·7	11·0	10·6	10·5	7·4	10·5	11·0	10·7	11·1	11·2	11·0	11·1
Zr	98·8	102·6	96·3	94·3	67·7	97·0	100·4	99·2	104·1	99·5	98·7	102·5
Hf	2·60	2·79	2·63	2·46	1·82	2·63	2·68	2·68	2·85	2·57	2·61	2·72
Sm	3·60	3·76	3·58	3·52	2·69	3·53	3·71	3·60	3·77	3·57	3·56	3·57
Eu	1·32	1·35	1·31	1·30	1·08	1·30	1·34	1·31	1·36	1·34	1·32	1·32
Gd	4·81	5·07	4·83	4·60	3·72	4·77	4·94	4·90	5·13	4·62	4·59	4·71
Tb	0·83	0·88	0·84	0·80	0·66	0·83	0·86	0·85	0·89	0·79	0·79	0·80
Dy	5·66	5·98	5·67	5·38	4·51	5·65	5·79	5·79	6·06	5·33	5·28	5·39
Ho	1·18	1·25	1·19	1·12	0·95	1·19	1·21	1·22	1·27	1·10	1·10	1·13
Er	3·45	3·66	3·47	3·26	2·79	3·46	3·54	3·55	3·73	3·21	3·19	3·29
Tm	0·49	0·52	0·49	0·46	0·39	0·49	0·51	0·51	0·53	0·45	0·45	0·47
Y	32·3	33·7	31·6	30·6	25·6	31·9	32·6	32·6	34·2	29·4	29·0	30·4
Yb	3·33	3·51	3·37	3·16	2·73	3·33	3·42	3·40	3·56	3·11	3·11	3·19
Lu	0·49	0·53	0·49	0·46	0·40	0·49	0·50	0·50	0·53	0·45	0·45	0·47
Ni	113	106	112	113	123	111	107	114	109	105	102	111
Sc	40·7	41·8	40·4	39·2	38·4	40·7	40·7	41·1	42·4	38·8	38·6	39·8

(continued)

Table 1: Continued

Cruise:	PS59						PS66				
Sample:	216-SG	218-36	218-SG	221-1	221-SG	223-8	214-2	214-7	214-5	214-3	214-1
Lat. (N):	83·07	83·08	83·08	83·26	83·26	83·3	82·97	82·97	82·97	82·97	82·97
Long. (W):	−6·04	−5·75	−5·75	−5·578	−5·578	−4·398	−4·92	−4·92	−4·92	−4·92	−4·92
WGR											
SiO_2	50·4	50·9	50·9	50·9	50·7	50·8	50·2	50·2	50·3	50·4	51·6
TiO_2	1·54	1·57	1·56	1·55	1·74	1·50	1·67	1·65	1·64	1·81	1·71
Al_2O_3	15·89	16·26	16·28	16·19	15·82	16·18	16·00	16·04	16·00	15·85	16·45
FeO	9·44	9·01	8·99	8·96	9·62	9·18	11·34	11·22	11·32	10·88	11·74
MnO	0·17	0·16	0·17	0·16	0·17	0·16	9·77	9·78	9·83	10·32	10·22
MgO	7·45	6·92	7·11	7·20	6·94	7·81	7·30	7·36	7·37	7·11	7·37
CaO	11·26	10·87	10·82	10·85	10·95	10·99	0·17	0·19	0·17	0·19	0·17
Na_2O	3·21	3·52	3·53	3·50	3·32	3·13	3·22	3·25	3·26	3·33	1·70
K_2O	0·17	0·25	0·24	0·23	0·21	0·22	0·16	0·17	0·17	0·18	0·15
P_2O_5	0·15	0·17	0·16	0·17	0·17	0·14	0·14	0·16	0·15	0·18	0·15
S	0·10	0·10	0·10	0·10	0·11	0·09	0·10	0·11	0·11	0·12	0·11
Cl	0·01	0·01	0·01	0·01	0·01	0·01	0·00	0·00	0·00	0·00	0·01
Total	99·74	99·71	99·84	99·86	99·73	100·17	100·03	100·14	100·30	100·34	101·39
Cs	0·03	0·05·5	0·06	0·06	0·04	0·03	0·03	0·03	0·03	0·03	0·03
Rb	2·39	4·32	4·40	4·35	3·22	3·36	2·25	2·22	2·26	2·10	2·34
Ba	30·4	52·3	52·0	51·0	43·0	48·4	26·7	25·4	26·0	24·6	28·0
Th	0·23	0·32	0·32	0·32	0·30	0·37	0·21	0·21	0·21	0·21	0·22
U	0·06	0·08	0·08	0·08	0·08	0·08	0·07	0·07	0·06	0·07	0·07
Nb	2·74	4·04	4·04	3·96	3·64	3·91	2·83	2·69	2·76	2·97	2·94
Ta	0·17	0·26	0·27	0·27	0·22	0·27	0·17	0·17	0·17	0·19	0·18
La	3·78	4·83	4·80	4·72	4·97	4·73	4·13	3·94	4·01	4·55	4·30
Ce	11·3	13·6	13·5	13·4	14·4	11·7	12·81	12·09	12·41	14·15	13·39
Pr	1·93	2·24	2·18	2·15	2·06	1·95	2·20	2·08	2·14	2·43	2·31
Sr	152	178	173	172	169	170	167	164	168	177	173
Pb	0·50	0·61	0·63	0·64	0·60	0·59	0·55	0·54	0·54	0·59	0·58
Nd	10·7	11·8	11·7	11·7	12·8	10·9	11·8	11·1	11·4	12·7	12·3
Zr	101·1	105·7	103·9	102·5	121·0	96·8	115	111	113	130	119
Hf	2·66	2·71	2·67	2·70	2·98	2·58	3·06	2·97	2·95	3·29	3·13
Sm	3·60	3·69	3·68	3·66	4·11	3·55	3·98	3·75	3·83	4·19	4·11
Eu	1·32	1·32	1·33	1·31	1·45	1·28	1·48	1·39	1·40	1·53	1·54
Gd	4·78	4·66	4·63	4·69	5·30	4·78	5·45	5·12	5·24	5·70	5·58
Tb	0·84	0·80	0·80	0·80	0·91	0·82	0·95	0·90	0·92	0·99	0·99
Dy	5·62	5·33	5·31	5·35	6·08	5·50	6·24	5·91	6·01	6·47	6·44
Ho	1·18	1·10	1·09	1·12	1·25	1·15	1·31	1·26	1·27	1·36	1·34
Er	3·42	3·19	3·19	3·19	3·63	3·30	3·84	3·71	3·73	3·99	4·00
Tm	0·49	0·45	0·45	0·46	0·52	0·47	0·53	0·52	0·52	0·56	0·55
Y	32·5	31·0	30·3	30·2	36·0	30·7	36·49	35·53	36·15	39·03	37·82
Yb	3·38	3·13	3·10	3·12	3·59	3·15	3·68	3·53	3·53	3·81	3·74
Lu	0·50	0·46	0·46	0·46	0·53	0·46	0·54	0·52	0·52	0·56	0·56
Ni	99	82	88	94	76	108	114	112	115	105	110
Sc	41·0	37·7	37·9	38·3	41·7	39·4	41·1	41·0	41·0	41·6	42·6

Samples were collected during several cruises: PS55, ARK XV/2 (1999); PS59, ARK XVII/2 (2001); PS66, ARK XX/2 (2004); HLY0102, USCGC *Healy*, Cruise 1 Leg 2 (2001).

to control the quality of the data acquisition. The average of repeated measurements of VG-2 is reported in Table 1. Reported analyses for samples are the average of at least three spots. For trace elements, LA-ICP-MS analyses were carried out with a New Wave UP-213 laser ablation system coupled with a Thermo Finnigan Element 2 ICP mass spectrometer. The beam diameter is 120 μm. NIST 612 and KL2-G were used to establish working curves for each element. The quality of the data was controlled by repeated measurement of ATHO-G reference glass (Table 1). Reported sample compositions are an average of several runs (at least three) on different chips of glass from each sample, to ensure that glass compositions are homogeneous and not affected by alteration.

For Sr–Nd–Hf–Pb isotopes, all samples were carefully hand picked from glassy pillow rims, crushed, sieved and rinsed in ultrapure deionized water. Hand-picked glasses were leached in 6 N HCl for 1 h on a hotplate prior to dissolution using an HF–HNO_3 mixture. Chemical separations were performed using the methods of Weis *et al.* (2005, 2006). Isotopic composition measurements were determined by thermal ionization mass spectrometry (TIMS) on a Finnigan Triton TI system (Sr, Nd) and by multi-collector (MC)-ICP-MS on a Nu Plasma Instruments system (Hf, Pb) at the Pacific Centre for Isotopic and Geochemical Research (PCIGR) at the University of British Columbia (UBC). Sr and Nd compositions were measured in static multi-collection mode on single Ta and double Re–Ta filaments, respectively. The measured ratios were corrected for mass fractionation using $^{86}Sr/^{88}Sr = 0{\cdot}1194$ and $^{146}Nd/^{144}Nd = 0{\cdot}7219$, respectively. External reproducibility was controlled by repeated analyses of NIST SRM 987 ($^{87}Sr/^{86}Sr = 0{\cdot}710256 \pm 16$, $n = 50$) for Sr and the La Jolla Nd standard ($^{143}Nd/^{144}Nd = 0{\cdot}511850 \pm 15$, $n = 50$) during the course of these analyses. Pb and Hf isotopic compositions were analyzed by static multi-collection on the Nu MC-ICP-MS system. The configuration for Pb isotopic analyses allows simultaneous collection of Pb (208, 207, 206 and 204) together with Tl (205 and 203), which is used to monitor and correct for instrumental mass discrimination (White *et al.*, 2000) and Hg (202), which is used to correct mass 204 for the potential presence of ^{204}Hg. The ^{204}Hg correction was made using natural abundances ($^{202}Hg = 0{\cdot}29863$ and $^{204}Hg = 0{\cdot}06865$ of total Hg) adjusted for instrumental mass fractionation using the $^{205}Tl/^{203}Tl$ ratio. To improve the reproducibility of the analytical conditions for the Pb isotopic analyses, and thus the precision, all sample solutions were analyzed with the same Pb/Tl ratios of ~4 as the NIST SRM 981 standards. To accomplish this, a small aliquot of each sample was analyzed by high-resolution (HR)-ICP-MS using an Element 2 system to determine the exact amount of Pb available for isotopic analysis. During the course of this study, the average of NST SRM 981 ($n = 72$) was $^{206}Pb/^{204}Pb = 16{\cdot}9407 \pm 36$, $^{207}Pb/^{204}Pb = 15{\cdot}4964 \pm 29$ and $^{208}Pb/^{204}Pb = 36{\cdot}7145 \pm 88$, which is comparable with triple spike values (Galer, 1999; Abouchami *et al.*, 2000). The total procedural Pb blank varied from 13 to 70 pg ($n = 8$) during the course of this study. The Hf isotope separations were carried out following an analytical procedure (Weis *et al.*, 2007) slightly modified from that of Patchett & Tatsumoto (1980) and Blichert-Toft *et al.* (1997). The configuration used to measure Hf isotopic ratios allows simultaneous collection of Hf isotopes (180, 179, 178, 177, 176 and 174) together with monitoring of Lu at mass 175 and Yb at mass 172, which allows interference corrections to be applied to masses 174 and 176 respectively. Hf isotope measurements were normalized for fractionation to a $^{179}Hf/^{177}Hf$ ratio of 0·7325 using an exponential correction. During the period of data collection, the JMC-475 Hf standard gave an unweighted mean for $^{176}Hf/^{177}Hf$ of $0{\cdot}282159 \pm 17$ ($n = 185$); this is comparable with values $^{176}Hf/^{177}Hf = 0{\cdot}282160 \pm 10$ given by Blichert-Toft *et al.* (2005). The standard was run every two samples to monitor instrument stability through time (Weis *et al.* 2007). The good external reproducibility (60 ppm) on the standard analyses indicates that no drift was observed. In Supplementary Data Table 1 (available for downloading at http://www.petrology.oxfordjournals.org), we report results for duplicate analyses of several samples.

RESULTS

Major elements

The Central Lena Trough (CLT) samples are highly unusual for MORB because they are relatively rich in K_2O, SiO_2 and Al_2O_3, with MgO of 5·05–6·48 wt %, SiO_2 of 51·1–51·8 wt %, Al_2O_3 of 18·12–18·44 wt %, Na_2O of 4·00–4·29 wt %, K_2O of 1·00–1·98 wt %, TiO_2 of 1·55–2·22 wt % and FeO* of 6·52–6·79 wt % (Table 1 and Fig. 2). Their Mg-number [molar $Mg/(Mg + Fe^{2+})$] ranges from 0·60 to 0·66. They are *ne*-normative and plot at the border between the trachy-basalt and basaltic trachy-andesite fields on a standard $Na_2O + K_2O$ vs SiO_2 (TAS) plot (Le Bas & Streckeisen, 1991). They are among the most alkali-rich samples ever dredged from a mid-ocean ridge setting. Only a few samples from the SWIR, mainly located on the Narrowgate segment (15°E), have similarly high $Na_2O + K_2O$ and K_2O/TiO_2 (3·31–6·50 and 0·35–0·79 respectively) (le Roex *et al.*, 1992; Standish *et al.*, 2008). Moreover, SWIR these high K_2O/TiO_2 MORB have lower Al_2O_3 (15·7–16·8 wt %), and SiO_2 (48·75–51·2 wt %) but higher FeO (7·03–9·80 wt %) for a given MgO (4·43–7·95 wt %) than the CLT samples; thus, their major element composition is not as extreme as that of the CLT lavas (Standish *et al.*, 2008). Similarly, lavas from the Mid-Atlantic Ridge (MAR) near the Bouvet Triple Junction also have low FeO (~6 wt %) and

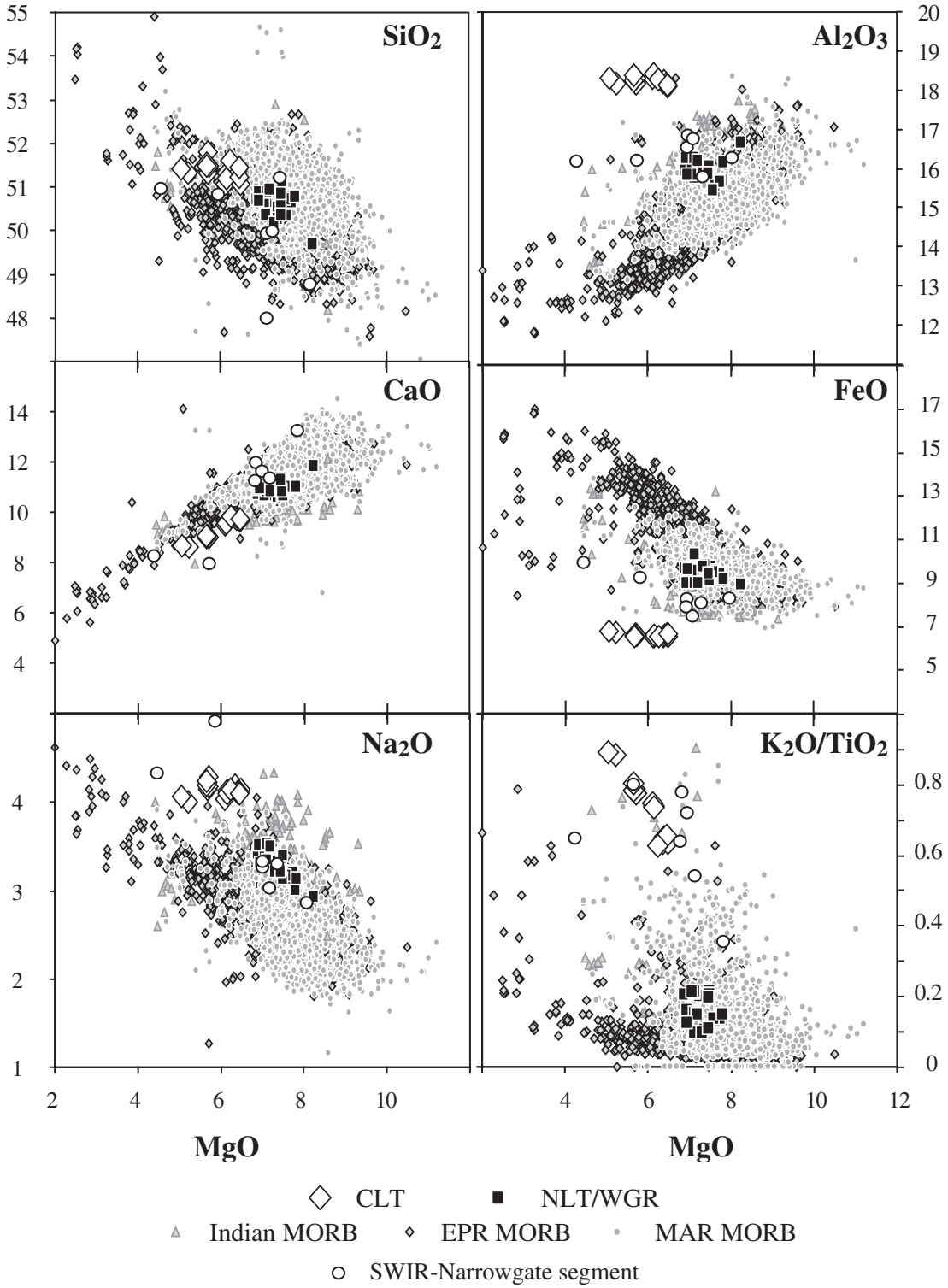

Fig. 2. Major element variation (wt %) vs MgO (wt %). CLT and NLT–WGR lavas are compared with East Pacific Rise (EPR), Mid-Atlantic Ridge (MAR) and Indian MORB (Petdb database, www.Petdg.org) and SWIR Narrowgate segment lavas (Standish *et al.*, 2008).

high Na_2O (>3·5 wt %), but they are richer in SiO_2 (>57 wt %) and poorer in CaO (<7 wt %) than the CLT lavas (Kamenetsky *et al.*, 2001). The CLT lavas are thus distinct from the lavas from the MAR near the Bouvet Triple Junction.

It is important to note that although the CLT samples are alkali basalt in composition, they are not chemically similar to what is commonly known as enriched (E)-MORB. E-MORB with high alkali contents generally have low SiO_2 (~49%) and Al_2O_3 (~15%) and have iron contents within the normal MORB range (9–11 wt % FeO_T) (Kamenetsky *et al.*, 1998), which the Central Lena Trough basalts do not; they are richer in SiO_2 and Al_2O_3 and poorer in iron for a given alkali content than any E-MORB yet reported. The CLT lavas thus represent a basalt composition that is apparently unique on the ocean floor.

Samples from the Northern Lena Trough and westernmost Gakkel Ridge (NLT–WGR) ($n = 37$) form a single compositional group and have more typical MORB compositions. They have MgO of 6·63–8·24 wt %, SiO_2 of 49·41–51·03 wt %, Al_2O_3 of 15·42–17·45 wt %, Na_2O of 2·94–3·54 wt %, K_2O of 0·07–0·66 wt % and FeO* of 8·94–10·32 wt % (Fig. 2). The Mg-number is nearly constant (0·57–0·65). Sample 219-2 has a somewhat similar major element composition to the CLT basalts with higher Al_2O_3 and K_2O/TiO_2 than the NLT/WGR basalts, but with lower SiO_2. It is *ne*-normative, like the CLT samples, whereas all of the other northern Lena Trough samples are *hy*-normative and plot in the basalt field of the TAS diagram.

Trace elements

The CLT basalts are enriched in all incompatible trace elements compared with normal (N)-MORB, with high La/Sm (2·3–2·8), Ba/Th (248–416), Ba/Nb (16·9–18·2) and $(Dy/Yb)_{PM}$ ratios (1·2–1·3). However, they are particularly enriched in the alkali elements K, Rb, Ba, Nb and Ta (Table 1). The CLT lavas are ~30 times richer in Ba and Rb and ~6 times richer in Nb and Ta than average N-MORB (Hofmann, 1988), and are the most K, Rb, Ba, Nb and Ta enriched lavas yet sampled from the global mid-ocean ridge system. They have positive Nb, Sr, Zr, Hf anomalies in primitive mantle normalized trace element diagrams (Hofmann, 1988) (Fig. 3) and unusual strong negative Th and U anomalies, although Th and U concentrations are between 0·70 and 1·3 ppm and between 0·20 and 0·42 ppm respectively. Moreover, they have very unusual trace element ratios compared with N-MORB, with very low Ba/Rb (9·4 ± 0·4) and Nb/Ta (14·6 ± 0·5) and very high Nb/U (65–76) and Ba/Nb (16·9–18·2). Although they have very low Ba/Rb, the samples are very fresh

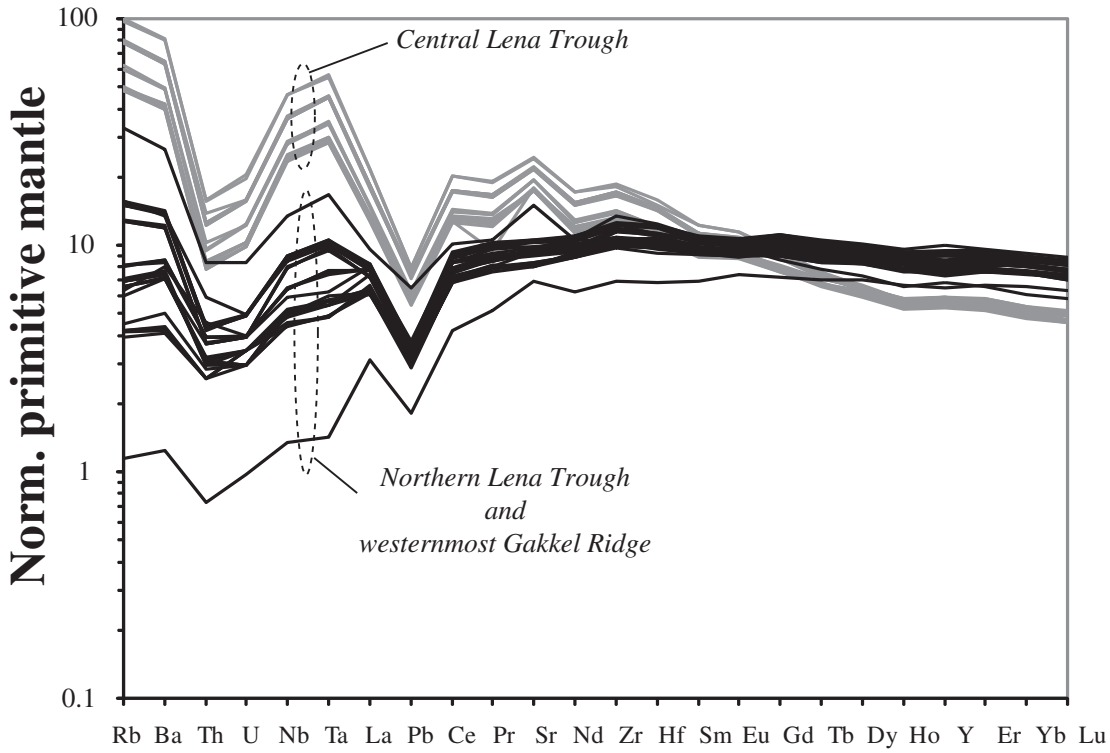

Fig. 3. Primitive mantle normalized trace element patterns; normalization constants from Hofmann (1988). Grey lines correspond to Central Lena Trough samples; black lines to Northern Lena Trough–westernmost Gakkel Ridge samples.

looking under the binocular microscope and in thin section, showing no effect of seawater alteration.

The NLT–WGR basalts display more MORB-like trace element characteristics compared with the CLT lavas. Excluding sample PS66 219-2, they have Ba/Th ranging from 117 to 256, Ba/Rb (11·8 ± 1·8) and Nb/U (48·6 ± 10·9) similar to the N-MORB reference values (11·4 ± 0·2 and 47 ± 10, respectively); Hofmann, 1988), and a Nb/Ta of 14·9 ± 1·3. In addition, they have relatively low Nd/Pb (19·8 ± 1·9). Average La/Sm is 1·13 ± 0·25 and the middle rare earth element (MREE) to heavy REE (HREE) trace element pattern is basically flat; $(Dy/Yb)_{PM}$ is 1·10 ± 0·03 (Fig. 3). The Eu/Eu* ratio is slightly lower than unity (0·95 ± 0·05). Only sample 219-2 is different, with higher La/Sm, $(Dy/Yb)_{PM}$ and Eu/Eu* (1·6, 1·19 and 1·01 respectively), and Nb/Ta and Nb/U (13·7 and 48·5 respectively).

Sr–Nd–Pb–Hf isotopes

The Sr, Nd, Pb and Hf isotope ratios of the samples are reported in Table 2 and their variation illustrated in Fig. 4. The CLT lavas have $^{87}Sr/^{86}Sr$ ranging from 0·70361 to 0·70390 and $^{143}Nd/^{144}Nd$ between 0·51283 and 0·51290 (ε_{Nd} + 3·7 to +5·2). In comparison, the NLT–WGR lavas have lower $^{87}Sr/^{86}Sr$ (0·70306–0·70340) and higher $^{143}Nd/^{144}Nd$ (0·51302–0·51308; ε_{Nd} + 7·5 to +8·6). CLT and NLT–WGR lavas also have different Hf isotope compositions, with $^{176}Hf/^{177}Hf$ ranging from 0·28313 to 0·28322 (ε_{Hf} + 11·6 to +14·9) and from 0·28323 to 0·28325 (ε_{Hf} + 15·0 to +16·1) respectively. There are also significant differences in the range and variations of Pb isotopic compositions between the CLT and NLT–WGR lavas. Central Lena Trough lavas show greater Pb isotopic variations with values of $^{206}Pb/^{204}Pb$ of 17·752–17·884, $^{207}Pb/^{204}Pb$ of 15·410–15·423 and $^{208}Pb/^{204}Pb$ of 37·544–37·670. CLT lavas plot below the Northern Hemisphere Reference Line (NHRL) line on a $^{207}Pb/^{204}Pb$ vs $^{206}Pb/^{204}Pb$ plot, whereas lavas with a DUPAL signature plot above this line (Hart, 1984). The Northern Lena Trough samples display very homogeneous Pb isotopic compositions, with $^{206}Pb/^{204}Pb$ of 17·986–17·995, $^{207}Pb/^{204}Pb$ of 15·432–15·440 and $^{208}Pb/^{204}Pb$ of 37·778–37·795. The Northern Lena Trough group is also characterized by more radiogenic Pb isotopic compositions. Whereas the NLT–WGR group has very homogeneous Pb isotopic compositions, which are almost all within analytical error of each other, the CLT group defines linear arrays in $^{207}Pb/^{204}Pb$–$^{206}Pb/^{204}Pb$ space and in $^{208}Pb/^{204}Pb$–$^{206}Pb/^{204}Pb$ space. The NLT–WGR lava group lies on the linear array defined by the CLT lavas in the $^{208}Pb/^{204}Pb$ vs $^{206}Pb/^{204}Pb$ and $^{207}Pb/^{204}Pb$ vs $^{206}Pb/^{204}Pb$ plots. On an ε_{Nd} vs $^{206}Pb/^{204}Pb$ plot, the NLT–WGR samples do lie on the edge of the MAR MORB field, but the CLT samples fall well outside with much lower ε_{Nd} values (Fig. 4c).

DISCUSSION

Major elements

The major features distinguishing the CLT lavas from most MORB revolve around the extreme alkali enrichment of the lavas, both on an absolute basis and in comparison with other incompatible trace elements. Figure 2 shows that the majority of MORB samples have a K_2O/TiO_2 ratio of less than about 0·2, whereas the CLT magmas range up to nearly unity. This is significant, as neither low-degree partial melting nor crystal fractionation is capable of significantly increasing the K_2O/TiO_2 of a basaltic magma. The major elements thus indicate that the alkali enrichment of these samples must be a source effect. The CLT samples also display unusually high Al_2O_3 contents (18·12–18·44 wt %) (Fig. 2). They do not plot on the MAR MORB positive correlation for Al_2O_3 vs MgO (Fig. 2), and are clearly distinct from other MORB with higher Na_2O and K_2O/TiO_2 and low FeO (Fig. 2). High-Al lavas elsewhere in an oceanic context appear to be mostly restricted to ridges with slow spreading rates or close to fracture zones and ridge terminations (Eason & Sinton, 2006). However, these Al-rich lavas are usually low-K (<0·1 wt %), low-Si lavas (<50 wt %) and relatively MgO rich (>8 wt %), and are believed to be generated either by low degrees of partial melting or by high-pressure clinopyroxene fractionation (Michael & Cornell, 1998; Eason & Sinton, 2006). The CLT magmas thus differ from other oceanic high-Al magmas.

Fractional crystallization and partial melting

One explanation for the unique characteristics of the CLT magmas compared with the NLT–GR MORB could be the crystallization process. High-pressure clinopyroxene fractionation (~5 kbar) might potentially explain the high Al_2O_3 and low CaO contents of the CLT lavas. However, such clinopyroxene fractionation does not explain the high K_2O/TiO_2, or the negative correlation between Sc and $^{206}Pb/^{204}Pb$ or $^{143}Nd/^{144}Nd$, or between K_2O/TiO_2 and isotope ratios (Fig. 5). Therefore, we conclude that the unique major element compositions of the CLT lava group cannot be explained by fractional crystallization.

The next step is to consider whether the CLT compositions are derived from an extreme partial melting process. The CLT lavas have similar major element compositions to those of experimental primary melts at low pressures and low degrees of partial melting of a peridotite with a high Al_2O_3 content (Baker *et al.*, 1995; Falloon *et al.*, 1997). These characteristics could be expected along an ultraslow-spreading ridge such as the Lena Trough. However, the K_2O contents and K_2O/Na_2O ratios are higher than those of any experimental partial melts thus far reported. It is also unlikely that even very low-degree

Table 2: Isotope compositions for Central and Northern Lena Trough lavas

	$^{206}Pb/^{204}Pb$	2σ	$^{207}Pb/^{204}Pb$	2σ	$^{208}Pb/^{204}Pb$	2σ	$^{87}Sr/^{86}Sr$	2σ	$^{143}Nd/^{144}Nd$	2σ	$^{176}Hf/^{177}Hf$	2σ	ε_{Hf}	ε_{Nd}
Central Lena Trough														
262-92	17·7776	0·0009	15·4122	0·0011	37·5656	0·0025	0·703619	0·000006	0·512857	0·000006	0·283173	0·000006	+13·19	+4·27
262-83	17·7839	0·0013	15·4143	0·0010	37·5735	0·0025	0·703776	0·000010	0·512851	0·000009	0·283165	0·000004	+12·91	+4·32
262-35	17·7606	0·0007	15·4116	0·0007	37·5534	0·0017	0·703898	0·000006	0·512826	0·000006	0·283128	0·000004	+11·60	+3·67
262-34	17·7522	0·0011	15·4102	0·0011	37·5444	0·0030	0·703771	0·000020	0·512829	0·000008	0·283137	0·000004	+11·90	+3·73
262-21	17·7839	0·0006	15·4145	0·0006	37·5779	0·0031	0·703757	0·000008	0·512853	0·000006	0·283169	0·000006	+13·05	+4·19
261-71	17·8776	0·0011	15·4221	0·0009	37·6638	0·0025	0·703646	0·000010			0·283216	0·000004	+14·71	
261-5	17·8606	0·0011	15·4193	0·0011	37·6430	0·0028	0·703638	0·000010	0·512893	0·000007	0·283207	0·000004	+14·41	+4·98
261-1	17·8615	0·0005	15·4198	0·0005	37·6461	0·0014	0·703626	0·000008			0·283207	0·000006	+14·39	
261-47	17·8802	0·0005	15·4225	0·0005	37·6690	0·0013	0·703611	0·000008	0·512901	0·000007	0·283221	0·000005	+14·90	+5·13
261-17	17·8838	0·0011	15·4222	0·0013	37·6695	0·0026	0·703649	0·000010	0·512903	0·000006	0·283211	0·000005	+14·55	+5·17
261-12	17·8620	0·0005	15·4201	0·0004	37·6458	0·0012	0·703640	0·000008	0·512898	0·000011	0·283222	0·000006	+14·92	+5·06
Northern Lena Trough														
217-5	17·9876	0·0011	15·4316	0·0012	37·7776	0·0032	0·703371	0·000001	0·513036	0·000008	0·283225	0·000006	+15·01	+7·76
217-9	17·9931	0·0013	15·4364	0·0011	37·7887	0·0033	0·703340	0·000010	0·513031	0·000009	0·283244	0·000005	+15·70	+7·67
217-8	17·9949	0·0008	15·4373	0·0009	37·7940	0·0025	0·703367	0·000009	0·513059	0·000008				+8·21
217-7	17·9931	0·0018	15·4386	0·0015	37·7930	0·0039	0·703369	0·000012	0·513037	0·000007	0·283240	0·000004	+15·57	
217-6	17·9922	0·0017	15·4379	0·0012	37·7913	0·0033	0·703377	0·000014	0·513031	0·000008	0·283236	0·000004	+15·41	+7·67
217-3	17·9947	0·0018	15·4373	0·0014	37·7949	0·0037	0·703347	0·000009	0·513024	0·000008	0·283246	0·000008	+15·75	+7·53
217-1	17·9942	0·0011	15·4376	0·0010	37·7894	0·0046	0·703395	0·000016			0·283242	0·000005	+15·63	
219-1	17·9858	0·0006	15·4398	0·0005	37·7879	0·0014	0·703348	0·000007	0·513041	0·000006	0·283239	0·000007	+15·52	+7·86
214-2	17·9938	0·0011	15·4362	0·0009	37·7907	0·0042	0·703057	0·000022	0·513080	0·000012				+8·62
217-4	17·9938	0·0006	15·4377	0·0005	37·7949	0·0013			0·513032	0·000011	0·283239	0·000005	+15·52	+7·68

External reproducibility was controlled by repeated analyses of NIST SRM 987 ($^{87}Sr/^{86}Sr = 0{\cdot}710256 \pm 16$), of La Jolla Nd standard ($^{143}Nd/^{144}Nd = 0{\cdot}511850 \pm 15$), of NIST SRM 981 ($^{206}Pb/^{204}Pb = 16{\cdot}9407 \pm 36$, $^{207}Pb/^{204}Pb = 15{\cdot}4964 \pm 29$, $^{208}Pb/^{204}Pb = 36{\cdot}7145$), of JMC-475 ($^{176}Hf/^{177}Hf = 0{\cdot}282159 \pm 17$). Pb isotope data were normalized to NIST SRM 981 values given by Abouchami *et al.* (2000).

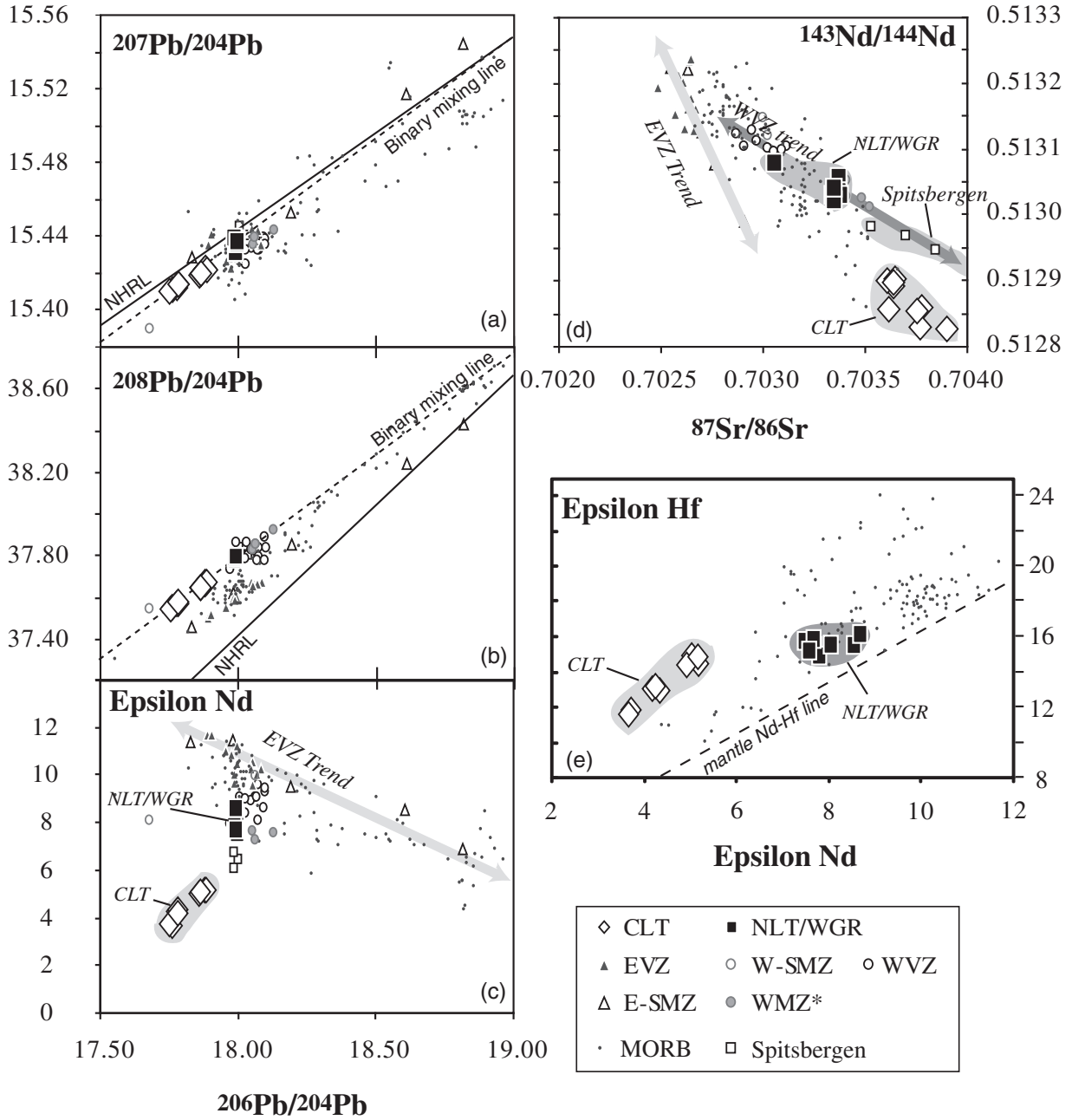

Fig. 4. (a) and (b) $^{207}Pb/^{204}Pb$ and $^{208}Pb/^{204}Pb$ vs $^{206}Pb/^{204}$ Pb, showing CLT and NLT–WGR composition compared with Gakkel Ridge lavas (Goldstein *et al.*, 2008), Quaternary basalts from Spitsbergen (Ionov *et al.*, 2002) and MAR MORB (www.Petdb.org). (c) ε_{Nd} vs $^{206}Pb/^{204}Pb$. (d) $^{143}Nd/^{144}Nd$ vs $^{87}Sr/^{86}Sr$ modified from Goldstein *et al.* (2008). (e) ε_{Hf} vs ε_{Nd}, with MAR MORB (Blichert-Toft *et al.*, 2005) and mantle Nd–Hf line (Chauvel *et al.*, 2001) indicated. Nomenclature for Gakkel Ridge lavas is after Goldstein *et al.* (2008): EVZ, eastern volcanic zone; WVZ, western volcanic zone; SMZ, sparsely magmatic zone. SMZ lavas show affinities to those in the adjacent WVZ and EVZ. W-SMZ and E-SMZ refer to lavas in the SMZ having isotopic affinities to the WVZ and EVZ, respectively. Samples labelled WVZ* were dredged from near the WVZ–SMZ boundary and follow the WVZ isotope trend but not the WVZ chemical trends.

partial melting of a peridotite composition alone could generate the high K_2O/TiO_2 values observed, because even at very low melting degrees, K is not sufficiently enriched (Baker *et al.*, 1995; Laporte *et al.*, 2004). A strong argument against the low-degree partial melting hypothesis for the major element composition is the existence of correlations between major elements and radiogenic isotopes (Figs 5 and 6). Because isotope ratios are the best source tracers and are not affected by partial melting or crystallization processes, correlations between major elements

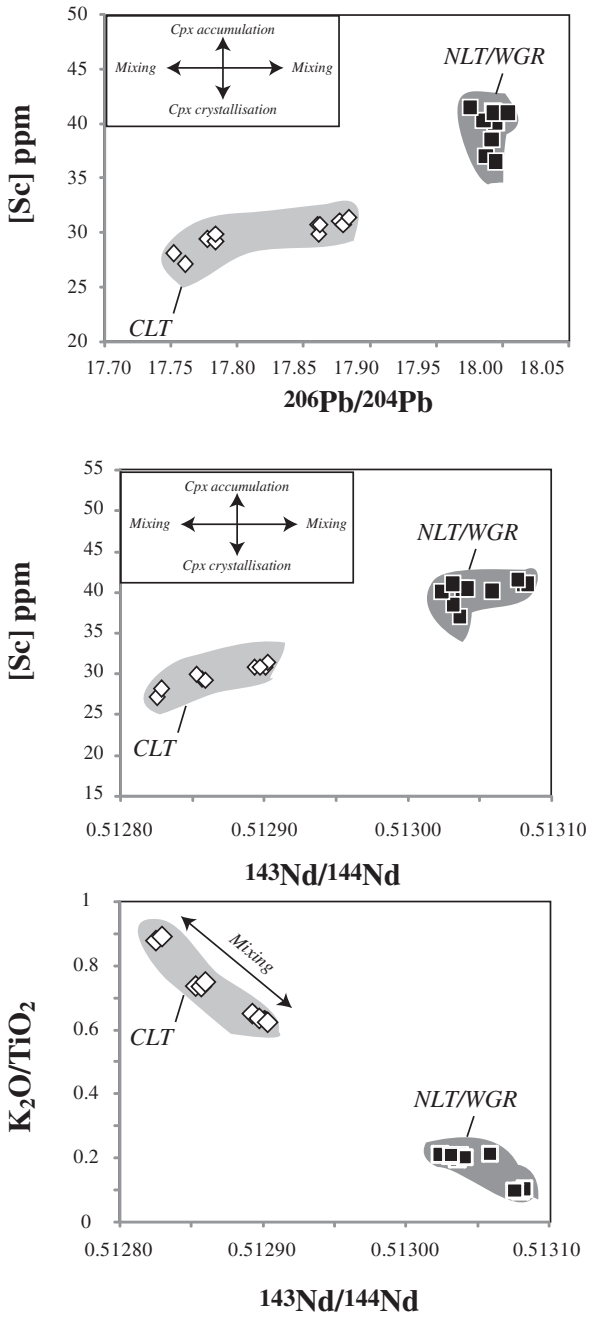

Fig. 5. CLT and NLT–WGR lavas are compared in diagrams of Sc vs $^{206}Pb/^{204}Pb$ and Sc vs $^{143}Nd/^{144}Nd$ to test if the low Sc concentrations in CLT lavas are due to clinopyroxene fractionation. Because $^{206}Pb/^{204}Pb$ and $^{143}Nd/^{144}Nd$ variations are related to the source, the positive correlation between Sc and $^{206}Pb/^{204}Pb$ suggests that Sc variations are also related to a binary mixing process. CLT and NLT–WGR are also compared in a K_2O/TiO_2 vs $^{143}Nd/^{144}Nd$ diagram.

and isotopes (e.g. K_2O/TiO_2 vs $^{143}Nd/^{144}Nd$) suggest that distinct major element compositions are also linked to different magma sources. The unusual major element composition of the CLT lavas is thus generated neither by low-degree partial melting of a normal MORB source mantle nor by a high-pressure crystallization process from a normal MORB.

Comparison to Gakkel Ridge Data

The Lena Trough and westernmost Gakkel Ridge lavas (Goldstein *et al.*, 2008) were generated along Arctic spreading centers near Spitsbergen Island where Quaternary volcanism has been described by Ionov *et al.* (2002). The CLT, NLT–WGR, Gakkel Ridge and Spitsbergen lavas all plot on the same line in $^{207}Pb/^{204}Pb$ and $^{208}Pb/^{204}Pb$ vs $^{206}Pb/^{204}Pb$ plots (Fig. 4a and b). In addition, the NLT–WGR lavas plot on the Western Volcanic Zone trend (WVZ trend) defined by the Gakkel WVZ lavas (Goldstein *et al.*, 2008) for $^{87}Sr/^{86}Sr$ vs $^{143}Nd/^{144}Nd$ and ε_{Nd} vs $^{206}Pb/^{204}Pb$. These WVZ trends point towards the Spitsbergen basalt field (Ionov *et al.*, 2002) (Fig. 4d). In contrast, the CLT lavas do not plot on these WVZ trends for $^{87}Sr/^{86}Sr$ vs $^{143}Nd/^{144}Nd$ or for ε_{Nd} vs $^{206}Pb/^{204}Pb$ as they have lower $^{143}Nd/^{144}Nd$ for a given $^{87}Sr/^{86}Sr$ compared with the Spitsbergen samples. They also have a significantly lower ε_{Nd} for a given $^{206}Pb/^{204}Pb$ (Fig. 4c). At the same time, these CLT lavas have higher ε_{Hf} than MAR MORB at a given ε_{Nd} and plot above the mantle Hf–Nd line, whereas the NLT–WGR lavas plot within the MAR MORB field (Fig. 4e). Thus the CLT lavas occupy a more extreme position in Sr–Nd–Pb–Hf isotopic space than any of the Gakkel or Spitsbergen basalts, suggesting a major contribution from a low U/Pb, light REE (LREE) and alkali enriched component that is not present in any of these other source regions and does not lie on the global MORB–OIB (ocean island basalt) Nd–Hf isotopic array (Blichert-Toft *et al.*, 2005).

Binary mixing

The major characteristics of the CLT data can be produced by a process of binary mixing between melts of disparate sources. There is a positive correlation between CaO and $^{143}Nd/^{144}Nd$ for the CLT lavas (Fig. 6). Because crystallization and melting processes do not fractionate $^{143}Nd/^{144}Nd$, we deduce from the CaO–$^{143}Nd/^{144}Nd$ correlation that the CaO variation is related to a mixing process. We observe a similar correlation between CaO and Sr–Hf–Pb isotopes, and between both MgO and K_2O and Sr–Nd–Pb–Hf isotopes. From these correlations between major elements and isotopes, we suggest that the unique major element composition of the CLT lavas is generated by a binary mixing process. In addition to major element–isotope correlations, linear correlations in Pb–Pb isotope diagrams are also interpreted as reflecting a binary mixing process. We also observe linear correlations in diagrams where trace element ratios with the same denominators are on both axes; for example, Ba/La vs Sm/La or Ni/La vs Ba/La (Figs 7 and 8). All these linear correlations are interpreted as reflecting a binary mixing process.

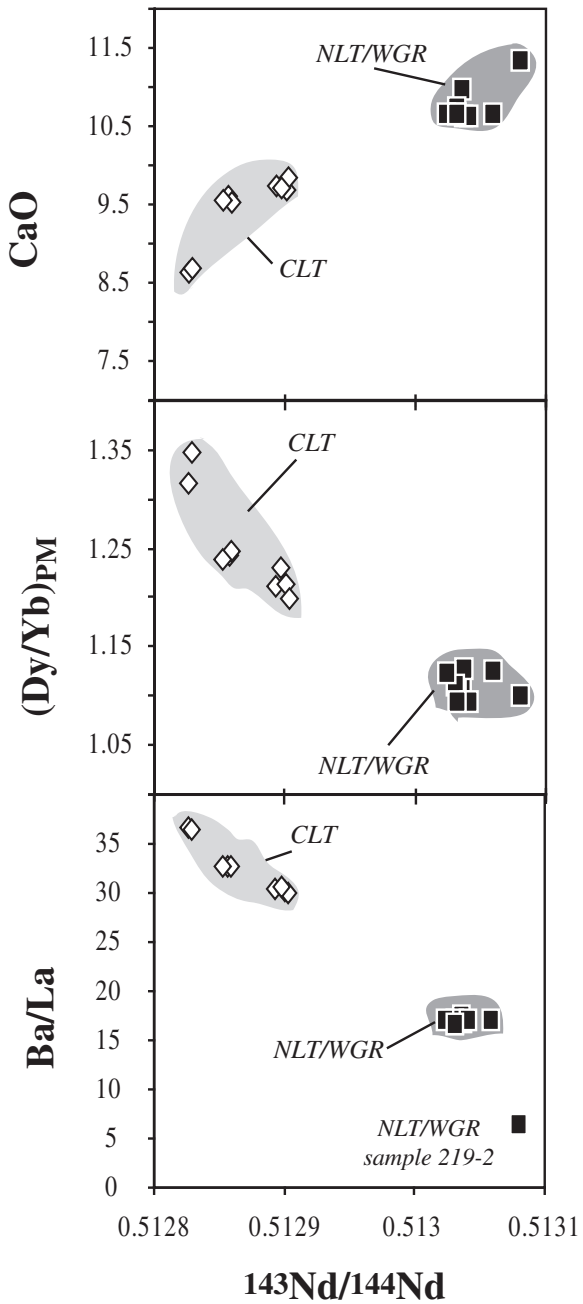

Fig. 6. CaO, $(Dy/Yb)_{PM}$ and Ba/La vs $^{143}Nd/^{144}Nd$. In these diagrams, $^{143}Nd/^{144}Nd$ is used as a source proxy because isotope ratios are not modified by crystallization or melting processes. $(Dy/Yb)_{PM}$ is used as a proxy to test if garnet is a residual phase in the source. High $(Dy/Yb)_{PM}$ suggests the presence of residual garnet in the source. Ba/La is used as a proxy for source composition because of the similar behavior of La and Ba during magmatic processes. CaO contents are classically used to investigate crystallization processes. However, for CLT lavas, correlation between CaO and $^{143}Nd/^{144}Nd$ suggests that the CaO content is related to the source composition.

Origin of mantle components

We have thus far concluded that the geochemical variations in major and trace elements and radiogenic isotopes of the CLT lavas are generated by a binary mixing process. The next step is to identify the nature of the end-member mixing components.

In a plot of Ni/La vs Ba/La (Fig. 8), the CLT lavas define a linear correlation between an N-MORB reference value (Hofmann, 1988) at one end and a component with high Ba/La and low Ni/La. We therefore assume that one of the end-members is MORB-like, and focus instead on the origin of the second component, which has high Ba/La and low Ni/La. For simplification, we call this high Ba/La ratio component, component (A), and the MORB-like end-member component (B). Based on correlations between major elements and radiogenic isotopes (e.g. MgO or CaO vs $^{143}Nd/^{144}Nd$), we conclude that component (A) has low MgO (<5 wt %) and CaO (<8·6 wt %), high K_2O (> 2 wt %), and high P_2O_5 (>0·3 wt %). Because component (A) has low MgO, we infer that it has very low Ni (the limit being Ni/La or Ni/TiO_2 ~0). Therefore we investigate linear correlations between Ni/TiO_2 vs X/TiO_2, where X is each major element; by using two-error least-squares regression methods we constrain the X/TiO_2 composition by extrapolating the correlation lines to the zero intercept of Ni/TiO_2 (Fig. 8). Although a major or trace element ratio of zero is, of course, unrealistic, this approach can be used to estimate the extreme bounds on the major and trace element ratios of the second component. There are rough linear correlations ($r^2>0·6$) for X/TiO_2 vs Ni/TiO_2, where X is a major element. From these correlations we calculate X/TiO_2 for each major element (SiO_2, MgO, FeO, CaO, Al_2O_3, Na_2O, K_2O) and we deduce that component (A) has $SiO_2/FeO = 7·51$, $FeO/MgO = 1·9$, $CaO/Al_2O_3 = 0·39$, $K_2O/TiO_2 = 1·05$ and $K_2O/Na_2O = 0·93$. These compositions are clearly distinct from those used in experimental studies investigating mafic lithologies in the mantle (Kogiso *et al.*, 2004). From these ratios and by assuming that component (A) is silica-rich (SiO_2 >52 wt %, higher than most CLT Si-rich lavas), we can deduce that it has FeO >7 wt % and thus MgO <3·6 wt %, and is ultra-potassic (K_2O/Na_2O >0·5), with a high Al content (>18·29 wt %). Therefore we infer that component (A) has characteristics similar to highly potassic melts of the shoshonite series, with $K_2O \approx Na_2O$ (Morrison, 1980) comparable with magma compositions observed in continental rift zones (Wilson & Downes, 1992).

Using a similar approach, we use linear correlations between X/Y vs isotope ratios, where X is a trace element and Y is Sr, Nd, Pb or Hf, to determine the isotopic composition of component (A) (Fig. 8). By extrapolating the correlation lines to the zero intercept of X/Y, we calculate the following isotope compositions for

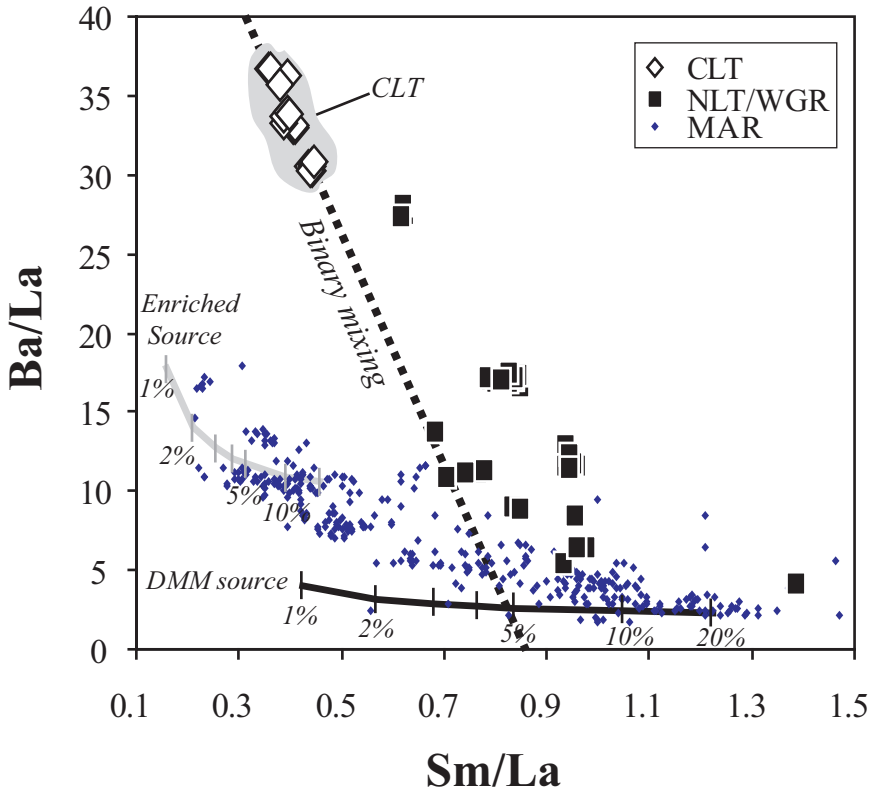

Fig. 7. Ba/La vs Sm/La diagram in which CLT, NLT–WGR and MAR MORB are compared. Sm/La is used as a proxy for the degree of partial melting and Ba/La is used as a proxy for the enrichment of the source. Two melting curves are shown: (1) with a DMM source composition with La = 0·237 ppm, Ba = 0·54 ppm, Sm = 0·388 ppm; (2) with an enriched source with La = 0·737 ppm, Ba = 7·54 ppm, Sm = 0·392 ppm and similar starting and modal compositions given by Donnelly *et al.* (2004). A regression line through the CLT data corresponding to a binary mixing line is also indicated (dashed line).

component (A): $^{87}Sr/^{86}Sr = 0{\cdot}70396$ ($r^2 = 0{\cdot}78$), $^{143}Nd/^{144}Nd = 0{\cdot}51277$ ($r^2 = 0{\cdot}91$), $^{206}Pb/^{204}Pb = 17{\cdot}6501$ ($r^2 = 0{\cdot}79$), $^{207}Pb/^{204}Pb = 15{\cdot}4017$ ($r^2 = 0{\cdot}78$), $^{208}Pb/^{204}Pb = 37{\cdot}4490$ ($r^2 = 0{\cdot}78$) and $^{176}Hf/^{177}Hf = 0{\cdot}28307$ ($r^2 = 0{\cdot}91$). These calculated isotope compositions represent an upper bound but are nevertheless close to the CLT field, suggesting a strong contribution of component (A) to the CLT geochemical signature (Fig. 4).

From these isotope characteristics, it is clear that component (A) cannot be derived from the depleted MORB mantle (DMM). This is also confirmed by trace element ratios used as a proxy for the depleted mantle source, such as Nb/U (68 ± 2; MORB = 45·74), Ba/Th (371 ± 68; MORB = 86·04) and Rb/Ba ($0{\cdot}1073 \pm 0{\cdot}0079$; MORB = 0·0874 (Salters & Stracke, 2004)). All the geochemical characteristics for component (A) are clearly distinct from the classic depleted mantle component often observed in OIB or MORB (Hofmann, 2003). Given that component (A) has a low MgO and Ni content, and very high inferred K and other alkali element contents, it most probably represents a melt derived from an exotic source component.

Constraints on the mineralogical composition of the Lena Trough mantle source

Given the high K_2O/TiO_2 of component (A), we suggest that it is derived from melting of a phlogopite- or K-rich amphibole-bearing source. As a result of the high affinity of K, Sr and Ba for amphibole and phlogopite [$D^{Ba}_{amphibole} = 0{\cdot}12$, $D^{Sr}_{amphibole} = 0{\cdot}28$ (Brenan *et al.*, 1995), $D^{Ba}_{phlogopite} = 3{\cdot}3$ and $D^{Sr}_{phlogopite} = 0{\cdot}21$ (Green *et al.*, 2000)] the breakdown of these phases during partial melting produces a high K, Sr, Ba melt (Ionov & Hofmann, 1995). These phases are often invoked to explain the presence of highly potassic magmas in continental rift zones (Wilson & Downes, 1992) or in convergent margins (Calmus *et al.*, 2003). The main geochemical characteristics of component (A) are consistent with amphibole or phlogopite partial melting, as it has been shown that the breakdown of amphibole to melt plus clinopyroxene may result in a melt poor in CaO, MgO and FeO and rich in SiO_2, Al_2O_3, K_2O, and Na_2O in comparison with the amphibole composition (Frey & Green, 1974). Amphibole breakdown could also explain the negative U–Th anomalies, as the

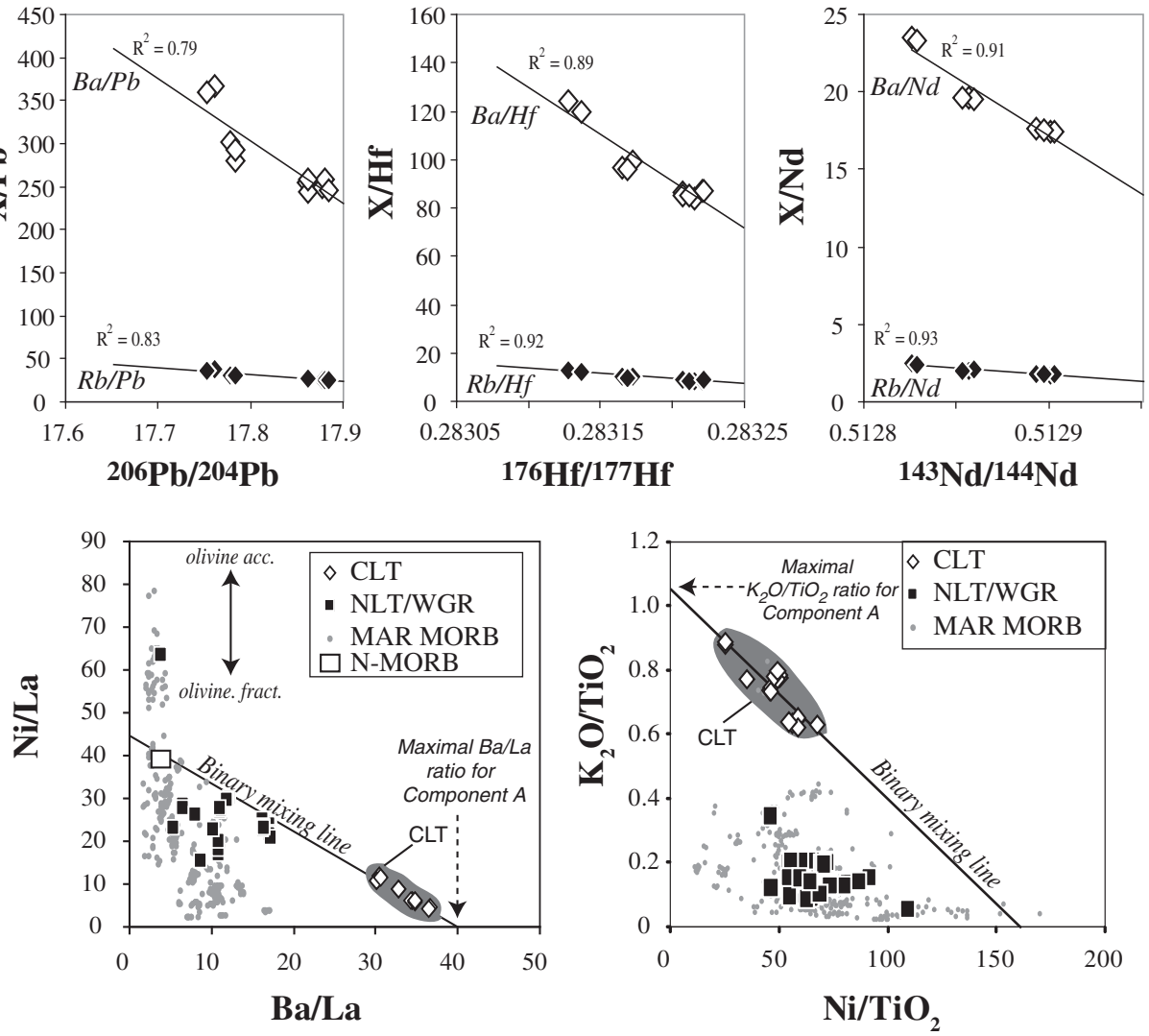

Fig. 8. Evidence for binary mixing: Rb/Pb and Ba/Pb vs $^{206}Pb/^{204}Pb$, Rb/Hf and Ba/Hf vs $^{176}Hf/^{177}Hf$, Ba/Nd and Rb/Nd vs $^{143}Nd/^{144}Nd$, Ni/La vs Ba/La and K_2O/TiO_2 vs Ni/TiO_2. All regression lines through the CLT data correspond to binary mixing lines. The line in the Ni/La vs Ba/La diagram is a regression line though the CLT data and forced to pass through the N-MORB reference value (Hofmann, 1988). Mid-Atlantic Ridge MORB data are shown for comparison.

Th–U contents in amphibole are very low (Latourrette *et al.*, 1995).

In addition, we have observed that the CLT lavas have higher Sm/Yb than average N-MORB [2·60 ± 0·64 for CLT and 1·31–1·49 for MORB (Hirschmann & Stolper, 1996)] and significantly lower Lu/Hf than N-MORB [0·07–0·1 for CLT lavas and 0·1–0·25 for MORB (Chauvel & Blichert-Toft, 2001)]. These features can be explained by the presence of garnet as a residual phase in the mantle source. The presence of garnet could explain the HREE depletion relative to the MREE, and is also suggested by the decoupling of Nd and Hf isotopes in the samples. Unusually radiogenic Hf at a specific value of $^{143}Nd/^{144}Nd$ might also be a signal for a source that experienced an ancient melting event in the presence of residual garnet (Blichert-Toft *et al.*, 2005) (Fig. 4). On the other hand, more radiogenic ε_{Hf} for a given ε_{Nd} might suggest that the source had experienced an event in the geological past that increased its Lu/Hf ratio to a greater extent than its Sm/Nd ratio; for example, by fluid addition, where Hf is less mobile than Lu, Sm and Nd. Such a fluid addition hypothesis would also be consistent with the high Na content in abyssal peridotites from the Lena Trough (Hellebrand & Snow, 2003) and might explain the high Ba/Nb (up to 18·2) and Ba/Th (up to 416) of the basalts, as Ba is more mobile in fluids than Nb and Th.

Thus, although we consider garnet as a likely residual phase in the mantle source of the CLT lavas, a fluid addition hypothesis cannot be completely ruled out.

Two rock types are possible candidates for the source of component (A). The first is a phlogopite or amphibole peridotite resulting from metasomatism of mantle peridotite by a hydrous fluid, as observed in a lithospheric thinning zone such as the Red Sea (Agrinier *et al.*, 1993). The second possibility is a phlogopite or amphibole pyroxenite such as a mica–amphibole–rutile–ilmenite–clinopyroxene (MARID) or glimmerite lithology (Gregoire *et al.*, 2002; Tappe *et al.*, 2006). Such rock-types are often invoked as sources for K-rich magmas such as lamproites, K-rich lamprophyres and shoshonitic lavas, which are similar to component (A) (Tappe *et al.*, 2008). Such K-rich lavas occur in rift zones and are the shallow-level expressions of K-rich metasomatism of the lithospheric mantle (Furman, 1995; Rogers *et al.*, 1998; Andersen, 2008; Rosenthal *et al.*, 2009). This could correspond to the geological setting of the Lena Trough if this zone is considered to be an ocean–continent transition zone where melting of the lithospheric mantle would be expected (Goldstein *et al.*, 2008). Melting of the lithospheric mantle has also been suggested by Nauret *et al.* (2010) from noble gas data. Those workers considered that an enriched component [like component (A)] might be degassed prior to mixing, or that the SCLM is precomponent sent as volumetrically small veins where there is He–Ne equilibrium between the veins and the surrounding peridotite matrix. Only the interpretation of Os isotopes in associated peridotites from the Lena Trough seems to contradict an SCLM contribution hypothesis (Lassiter & Snow, 2009). A lack of Nd–Sr isotopic overlap between lavas and peridotites was found beneath the western SWIR, by Salters & Dick (2002), and those workers have concluded that enriched heterogeneities, removed completely by melting, must have contributed to the compositions of the lavas, but are not represented in the compositions of the abyssal peridotites. A similar conclusion could be drawn for the Lena Trough. MARID or glimmerite sources are present in the mantle beneath Greenland (Coulson, 2003; Tappe *et al.*, 2008) and therefore might also be present in the central part of the Lena Trough. K-rich magmas can also occur close to recent or ancient convergent plate margins (Foley *et al.*, 1987), where continental crust or derived sediments are required in the mantle source (Nelson & Livieres, 1986; Stolz *et al.*, 1990), although this scenario does not correspond to the geological setting of the Lena Trough.

So far, we cannot establish conclusively how the phlogopite- or amphibole-bearing source was produced. Several models have proposed that phlogopite- or amphibole-rich veins could be formed at the base of the lithospheric mantle by reaction with rising fluids or melts (McKenzie, 1989; Vaughan & Scarrow, 2003; Tappe *et al.*, 2009). Such a source could account for the enriched component in the Gakkel Ridge lavas (Goldstein *et al.*, 2008), which could be linked to the alkalic volcanism on Spitsbergen. The logical location for such a hydrous source is the subcontinental lithospheric mantle, suggesting that despite contrary indications from the available Os isotope data (Lassiter & Snow, 2009), the central Lena basalts ultimately have a shallow lithospheric mantle origin.

Relationship between the CLT and the NLT magmas

The NLT magmas have the characteristics of N-MORB in terms of their major and trace element compositions (Figs 2 and 3). They have undergone fractional crystallization at shallow depths and they have similar Sr–Nd–Hf–Pb isotope characteristics to the WVZ Gakkel Ridge lavas (Fig. 4). Therefore we conclude that they were generated by the same process as the WVZ Gakkel Ridge lavas (Goldstein *et al.*, 2008). From the observations above and the differences in isotopic composition, we deduce that the NLT and CLT magmas were not derived from the same mantle source, nor from each other by fractional crystallization. This is shown by clear differences in K_2O/TiO_2, Nb/U and Nd/Pb ratios, which would not be expected to be affected by fractionation of basalt liquidus phases. The source of the NLT–WGR lavas, like that of the WVZ Gakkel ridge samples, appears to be formed by the addition of Spitsbergen SCLM to the ambient North Atlantic asthenosphere (Goldstein *et al.*, 2008). The CLT lavas are also formed by similar mixing processes, but the mineralogical and isotope composition of the SCLM end-member must be different to explain the fact that CLT lavas contain a significant melt fraction derived from a very different amphibole- or phlogopite-, (potentially garnet)-bearing mantle source. This difference implies a mineralogically heterogeneous upper mantle underlying the Lena Trough–Gakkel Ridge spreading system.

The Lena Trough mantle

In addition to the previous work on the Gakkel Ridge MORB (Goldstein *et al.*, 2008), we show here that the CLT lavas have a lithospheric mantle signature. This might also account for the origin of the southern hemisphere DUPAL-like isotopic anomaly observed in the Arctic Ocean (Mühe *et al.*, 1993, 1997; Goldstein *et al.*, 2008). However, notable differences are observed between the Gakkel Ridge MORB and the Central Lena Trough in terms of the strength of the SCLM signature, and the isotope compositions. These differences may originate from the variable composition of the lithospheric mantle in the Arctic region. Also, the strong influence of the K-rich component (A) is probably related to the restricted spreading rate in the central section of the Lena Trough. Because the spreading rate in the Lena Trough is effectively lower than that of the Gakkel Ridge, the degree of melting

in the mantle is depressed and thus a higher proportion of the very fertile source component melt is present in the CLT lavas. This explains why the amount of K-rich melt [component (A)] is higher in the CLT lavas compared with NLT–WGR and Gakkel Ridge MORB. We conclude that the geochemical composition of the erupted lavas is controlled by the heterogeneity of the underlying mantle and also directly by the local thermal structure of the lithosphere (McKenzie, 1989; Vaughan & Scarrow, 2003; Standish *et al.*, 2008). Similar interpretations have been used to explain specific SWIR MORB characteristics (Standish *et al.*, 2008).

So far, we have deduced that component (A) is derived from an amphibole- or phlogopite-bearing (and potentially garnet-bearing) mantle source that is clearly distinct from that beneath the Gakkel Ridge (Goldstein *et al.*, 2008). This suggests that the mineralogy of Arctic lithospheric mantle is highly heterogeneous. This has been suggested previously based on studies of mantle xenoliths from Spitsbergen (Ionov *et al.*, 2002). We envisage the Lena Trough mantle to contain volumetrically small phlogopite- or amphibole- (and potentially garnet)-bearing veins (Nauret *et al.*, 2010), which carry the signature of the SCLM. The geochemical and geological evidence suggests that the Lena Trough is an ocean–continent transition zone with a complex history as it is located in an oceanic domain of highly oblique spreading; however, the melts also share geochemical characteristics (high K) with continental rift lavas (Wilson & Downes, 1992). As a result of the opening of the Arctic–North Atlantic Ocean, the sub-continental lithospheric mantle beneath the Lena Trough was heated and the highly fertile component was melted, generating the component (A).

CONCLUSIONS

Basalts recovered from the ultraslow and highly oblique spreading Lena Trough have unique major, trace element and Sr–Nd–Pb–Hf isotope compositions, particularly those from the central part of the trough. Major and trace elements, as well as isotope ratios, can be explained by a binary mixing process between a MORB-like melt component, seen mainly in the NLT–WGR lavas, and a shoshonitic melt referred to as component (A), which is clearly observed in the CLT lavas. Component (A) is interpreted as deriving from a phlogopite- or amphibole- and possibly garnet-bearing source, which represents the SCLM. From the marked input of the SCLM component to the geochemistry of the CLT lavas, we define the Lena Trough as being an ocean–continent transitional boundary with very low melt productivity. Although the Lena Trough lavas have a unique geochemical composition, such magmatism would be expected to occur wherever ocean spreading initiates. The Lena Trough may therefore be considered as a reference locality for the earliest melt derived from shallow melting of rifted continental lithospheric mantle.

ACKNOWLEDGEMENTS

The authors wish to thank the Captain, crew and other scientific participants in PFS *Polarstern* ARK XX-2, the Alfred Wegener Institute for access to ship time on PFS *Polarstern*, and Hans Werner Schenke (AWI) for the use of previously unpublished bathymetric data. Thoughtful and thorough reviews by two anonymous reviewers greatly improved the paper. The authors thank C. Devey for the editorial work.

FUNDING

F. Nauret was supported by a post-doctoral fellowship at UBC, and analyses partly through D. Weis NSERC discovery grant. J. E. Snow was supported by grant OCE 0648567 from the National Science Foundation, and by the Deutsche Forschungsgemeinschaft and the Max Planck Society.

SUPPLEMENTARY DATA

Supplementary data for this paper are available at *Journal of Petrology* online.

REFERENCES

Abouchami, W., Galer, S. J. G. & Hofmann, A. W. (2000). High precision lead isotope systematics of lavas from the Hawaiian Scientific Drilling Project. *Chemical Geology* **169**, 187–209.

Agrinier, P., Mevel, C., Bosch, D. & Javoy, M. (1993). Metasomatic hydrous fluids in amphibole peridotites from Zabargad Island (Red Sea). *Earth and Planetary Science Letters* **120**, 187–205.

Andersen, T. (2008). Coexisting silicate and carbonatitic magmas in the Qassiarsuk Complex, Gardar Rift, Southwest Greenland. *Canadian Mineralogist* **46**, 933–950.

Baker, M. B., Hirschmann, M. M., Ghiorso, M. S. & Stolper, E. M. (1995). Compositions of near-solidus peridotite melts from experiments and thermodynamic calculations. *Nature* **375**, 308–311.

Blichert-Toft, J., Chauvel, C. & Albarède, F. (1997). Separation of Hf and Lu for high-precision isotope analysis of rock samples by magnetic sector multiple collector ICP-MS. *Contributions to Mineralogy and Petrology* **127**, 248–260.

Blichert-Toft, J., Agranier, A., Andres, M., Kingsley, R., Schilling, J. G. & Albarède, F. (2005). Geochemical segmentation of the Mid-Atlantic Ridge north of Iceland and ridge–hot spot interaction in the North Atlantic. *Geochemistry, Geophysics, Geosystems* **6**, doi:10.1029/2004GC000788.

Bown, J. W. & White, R. S. (1994). Variation with spreading rate of oceanic crustal thickness and geochemistry. *Earth and Planetary Science Letters* **121**, 435–449.

Brenan, J. M., Shaw, H. F., Ryerson, F. J. & Phinney, D. L. (1995). Experimental determination of trace-element partitioning between pargasite and a synthetic hydrous andesitic melt. *Earth and Planetary Science Letters* **135**, 1–11.

Calmus, T., Aguillon-Robles, A., Maury, R. C., Bellon, H., Benoit, M., Cotten, J., Bourgeois, J. & Michaud, F. (2003). Spatial

and temporal evolution of basalts and magnesian andesites ('bajaites') from Baja California, Mexico: the role of slab melts. *Lithos* **66**, 77–105.

Chauvel, C. & Blichert-Toft, J. (2001). A hafnium isotope and trace element perspective on melting of the depleted mantle. *Earth and Planetary Science Letters* **190**, 137–151.

Coulson, I. M. (2003). Evolution of the North Qoroq centre nepheline syenites, South Greenland: alkali–mafic silicates and the role of metasomatism. *Mineralogical Magazine* **67**, 873–892.

Debaille, V., Blichert-Toft, J., Agranier, A., Doucelance, R., Schiano, P. & Albarède, F. (2006). Geochemical component relationships in MORB from the Mid-Atlantic Ridge, 22–35°N. *Earth and Planetary Science Letters* **241**, 844–862.

Donnelly, K. E., Goldstein, S. L., Langmuir, C. H. & Spiegelman, M. (2004). Origin of enriched ocean ridge basalts and implications for mantle dynamics. *Earth and Planetary Science Letters* **226**, 347–366.

Eason, D. & Sinton, J. (2006). Origin of high-Al N-MORB by fractional crystallization in the upper mantle beneath the Galapagos Spreading Center. *Earth and Planetary Science Letters* **252**, 423–436.

Falloon, T. J., Green, D. H., O'Neill, H. S. C. & Hibberson, W. O. (1997). Experimental tests of low degree peridotite partial melt compositions: implications for the nature of anhydrous near-solidus peridotite melts at 1 GPa. *Earth and Planetary Science Letters* **152**, 149–162.

Foley, S. F., Venturelli, G., Green, D. H. & Toscani, L. (1987). The ultrapotassic rocks—characteristics, classification, and constraints for petrogenetic models. *Earth-Science Reviews* **24**, 81–134.

Frey, F. A. & Green, D. H. (1974). Mineralogy, geochemistry and origin of lherzolite inclusions in Victorian basanites. *Geochimica et Cosmochimica Acta* **38**, 1023–1059.

Furman, T. (1995). Melting of metasomatized subcontinental lithosphere—undersaturated mafic lavas from Rungwe, Tanzania. *Contributions to Mineralogy and Petrology* **122**, 97–115.

Galer, S. J. G. (1999). Optimal double and triple spiking for high precision lead isotopic measurement. *Chemical Geology* **157**, 255–274.

Goldstein, S. L., Soffer, G., Langmuir, C. H., Lehnert, K. A., Graham, D. W. & Michael, P. J. (2008). Origin of a 'Southern Hemisphere' geochemical signature in the Arctic upper mantle. *Nature* **453**, 89–93.

Green, T. H., Blundy, J. D., Adam, J. & Yaxley, G. M. (2000). SIMS determination of trace element partition coefficients between garnet, clinopyroxene and hydrous basaltic liquids at 2–7·5 GPa and 1080–1200°C. *Lithos* **53**, 165–187.

Gregoire, M., Bell, D. R. & Le Roex, A. P. (2002). Trace element geochemistry of phlogopite-rich mafic mantle xenoliths: their classification and their relationship to phlogopite-bearing peridotites and kimberlites revisited. *Contributions to Mineralogy and Petrology* **142**, 603–625.

Hart, S. R. (1984). A large-scale isotope anomaly in the Southern Hemisphere mantle. *Nature* **309**, 753–757.

Hellebrand, E. & Snow, J. E. (2003). Deep melting and sodic metasomatism underneath the highly oblique-spreading Lena Trough (Arctic Ocean). *Earth and Planetary Science Letters* **216**, 283–299.

Hirschmann, M. M. & Stolper, E. M. (1996). A possible role for garnet pyroxenite in the origin of the 'garnet signature' in MORB. *Contributions to Mineralogy and Petrology* **124**, 185–208.

Hofmann, A. W. (1988). Chemical differentiation of the Earth: the relationship between mantle, continental crust, and oceanic crust. *Earth and Planetary Science Letters* **90**, 297–314.

Hofmann, A. W. (2003). Sampling mantle heterogeneity through oceanic basalts: Isotopes and trace element. In: Carlson, R. W. (ed.) *The Mantle and Core*. Oxford: Elsevier–Pergamon, pp. 61–101.

Hofmann, A. W. & Hart, S. R. (1978). An assessment of local and regional isotopic equilibrium in the mantle. *Earth and Planetary Science Letters* **39**, 44–62.

Ionov, D. A. & Hofmann, A. W. (1995). Nb–Ta-rich mantle amphiboles and micas: Implications for subduction-related metasomatic trace element fractionations. *Earth and Planetary Science Letters* **131**, 341–356.

Ionov, D. A., Mukasa, S. B. & Bodinier, J.-L. (2002). Sr–Nd–Pb isotopic compositions of peridotite xenoliths from Spitsbergen: numerical modelling indicates Sr–Nd decoupling in the mantle by melt percolation metasomatism. *Journal of Petrology* **43**, 2261–2278.

Jokat, W. (2000). *The Expedition ARKTIS-XV/2 of 'Polarstern' in 1999. Alfred Wegener Institut for Polar and Marine Research. Berichte zur Polarforschung* **368**, 128.

Jokat, W., Ritzmann, O, Schmidt-Aursch, M. C., Drachev, S., Gauger, S. & Snow, J. E. (2003). Geophysical evidence for reduced melt production on the Arctic ultraslow Gakkel mid-ocean ridge. *Nature* **423**, 962–965.

Kamenetsky, V. S., Eggins, S. M., Crawford, A. J., Green, D. H., Gasparon, M. & Falloon, T. J. (1998). Calcic melt inclusions in primitive olivine at 43°N MAR: evidence for melt–rock reaction/melting involving clinopyroxene-rich lithologies during MORB generation. *Earth and Planetary Science Letters* **160**, 115–132.

Kamenetsky, V. S., Maas, R., Sushchevskaya, N. M., Norman, M. D., Cartwright, I. & Peyve, A. A. (2001). Remnants of Gondwanan continental lithosphere in oceanic upper mantle: Evidence from the South Atlantic Ridge. *Geology* **29**, 243–246.

Kogiso, T., Hirschmann, M. M. & Pertermann, M. (2004). High-pressure partial melting of mafic lithologies in the mantle. *Journal of Petrology* **45**, 2407–2422.

Laporte, D., Toplis, M. J., Seyler, M. & Devidal, J. L. (2004). A new experimental technique for extracting liquids from peridotite at very low degrees of melting: application to partial melting of depleted peridotite. *Contributions to Mineralogy and Petrology* **146**, 463–484.

Lassiter, J. C. & Snow, J. E. (2009). Os-isotope constraints on the origin of Lena Trough peridotites, Arctic Ocean: Asthenospheric mantle or continental lithosphere? *Geochimica et Cosmochimica Acta* **73**, A725–A725.

Latourrette, T., Hervig, R. L. & Holloway, J. R. (1995). Trace-element partitioning between amphibole, phlogopite, and basanite melt. *Earth and Planetary Science Letters* **135**, 13–30.

Le Bas, M. J. & Streckeisen, A. L. (1991). The IUGS systematic of igneous rocks. *Journal of the Geological Society, London* **148**, 825–833.

le Roex, A. P., Erlank, A. J. & Needham, H. D. (1981). Geochemical and mineralogical evidence for the occurrence of at least 3 distinct magma types in the FAMOUS region. *Contributions to Mineralogy and Petrology* **77**, 24–37.

le Roex, A. P., Dick, H. J. B. & Watkins, R. T. (1992). Petrogenesis of anomalous K-enriched MORB from the Southwest Indian Ridge—11°53′E To 14°38′E. *Contributions to Mineralogy and Petrology* **110**, 253–268.

Liu, C. Z., Snow, J. E., Hellebrand, E., Brugmann, G., Handt, A. V., Buchl, A. & Hofmann, A. W. (2008). Ancient, highly heterogeneous mantle beneath Gakkel ridge, Arctic Ocean. *Nature* **452**, 311–317.

McKenzie, D. (1989). Some remarks on the movement of small melt fractions in the mantle. *Earth and Planetary Science Letters* **95**, 53–72.

Michael, P., Thiede, J., Dick, H. J. *et al.* (2001). Results of the Arctic Mid-Ocean Ridge Expedition—AMORE 2001—seafloor spreading at the top of the world. *International Ridge-Crest Research* 57–60.

Michael, P. J. & Cornell, W. C. (1998). Influence of spreading rate and magma supply on crystallization and assimilation beneath mid-ocean ridges: Evidence from chlorine and major element

chemistry of mid-ocean ridge basalts. *Journal of Geophysical Research: Solid Earth* **103**, 18325–18356.

Morrison, G. W. (1980). Characteristics and tectonic setting of the shoshonite rock association. *Lithos* **13**, 97–108.

Mühe, R., Devey, C. W. & Bohrmann, H. (1993). Isotope and trace-element geochemistry of MORB from the Nansen–Gakkel Ridge at 86°North. *Earth and Planetary Science Letters* **120**, 103–109.

Mühe, R., Bohrmann, H., Garbe-Schonberg, D. & Kassens, H. (1997). E-MORB glasses from the Gakkel Ridge (Arctic Ocean) at 87°N: evidence for the Earth's most northerly volcanic activity. *Earth and Planetary Science Letters* **152**, 1–9.

Nauret, F., Moreira, M. & Snow, J. E. (2010). Rare gases in lavas from the ultraslow spreading Lena Trough, Arctic Ocean. *Geochemistry, Geophysics, Geosystems* **11**, Q0AC04.

Nelson, S. A. & Livieres, R. A. (1986). Contemporaneous calc-alkaline and alkaline volcanism at Sanganguey Volcano, Nayarit, Mexico. *Geological Society of America Bulletin* **97**, 798–808.

Patchett, P. J. & Tatsumoto, M. (1980). A routine high-precision method for Lu–Hf isotope geochemistry and chronology. *Contributions to Mineralogy and Petrology* **75**, 263–267.

Reid, I. & Jackson, H. R. (1981). Oceanic spreading rate and crustal thickness. *Marine Geophysical Researches* **5**, 165–172.

Rogers, N. W., James, D., Kelley, S. P. & De Mulder, M. (1998). The generation of potassic lavas from the eastern Virunga province, Rwanda. *Journal of Petrology* **39**, 1223–1247.

Rosenthal, A., Foley, S. F., Pearson, D. G., Nowell, G. M. & Tappe, S. (2009). Petrogenesis of strongly alkaline primitive volcanic rocks at the propagating tip of the western branch of the East African Rift. *Earth and Planetary Science Letters* **284**, 236–248.

Salters, V. J. M. & Dick, H. J. B. (2002). Mineralogy of the mid-ocean-ridge basalt source from neodymium isotopic composition of abyssal peridotites. *Nature* **418**, 68–72.

Salters, V. J. M. & Stracke, A. (2004). Composition of the depleted mantle. *Geochemistry, Geophysics, Geosystems* **5**, Q05B07, doi:10.1029/2003GC000597.

Snow, J. E., Hart, S. R. & Dick, H. J. B. (1994). Nd and Sr isotope evidence linking mid-ocean-ridge basalts and abyssal peridotites. *Nature* **371**, 57–60.

Snow, J. E. & Shipboard Scientific Party (2002). Petrogenesis of Crustal Rocks. In: Thiede, J. (ed.) *POLARSTERN ARKTIS XVII/2 Cruise Report. AMORE 2001 (Arctic Mid-Ocean Ridge Expedition)*, Bremerhaven: Alfred Wegener Institute for Polar and Marine Research **421**, 118.

Snow, J. E., Feldmann, H., Handt, A.v.d. *et al.* (2007). Petrologic and tectonic evolution of the Lena Trough and Western Gakkel Ridge. In: Budéus, G. & Lemke, P. (eds) *Reports on Polar and Marine Research*. Bremerhaven: Alfred Wegener Institute for Polar and Marine Research, pp. 153–208.

Standish, J. J., Dick, H. J. B., Michael, P. J., Melson, W. G. & O'Hearn, T. (2008). MORB generation beneath the ultraslow spreading Southwest Indian Ridge (9–25°E): Major element chemistry and the importance of process versus source. *Geochemistry, Geophysics, Geosystems* **9**, Q05004, doi:10.1029/2008GC001959.

Stolz, A. J., Varne, R., Davies, G. R., Wheller, G. E. & Foden, J. D. (1990). Magma source components in an arc–continent collision zone—the Flores–Lembata Sector, Sunda Arc, Indonesia. *Contributions to Mineralogy and Petrology* **105**, 585–601.

Tappe, S., Foley, S. F., Jenner, G. A., Heaman, L. M., Kjarsgaard, B. A., Romer, R. L., Stracke, A., Joyce, N. & Hoefs, J. (2006). Genesis of ultramafic lamprophyres and carbonatites at Aillik Bay, Labrador: A consequence of incipient lithospheric thinning beneath the North Atlantic craton. *Journal of Petrology* **47**, 1261–1315.

Tappe, S., Steenfelt, A., Heaman, L. M., Romer, R. L., Simonetti, A. & Muehlenbachs, K. (2008). The alleged carbonatitic–kimberlitic melt continuum: Contrary evidence from West Greenland. *Geochimica et Cosmochimica Acta* **72**, A934–A934.

Tappe, S., Heaman, L. M., Romer, R. L., Steenfelt, A., Simonetti, A., Muehlenbachs, K. & Stracke, A. (2009). Quest for primary carbonatite melts beneath cratons: A West Greenland perspective. *Geochimica et Cosmochimica Acta* **73**, A1314–A1314.

Vaughan, A. P. M. & Scarrow, J. H. (2003). K-rich mantle metasomatism control of localization and initiation of lithospheric strike-slip faulting. *Terra Nova* **15**, 163–169.

Weis, D., Kieffer, B., Maerschalk, C., Pretorius, W. & Barling, J. (2005). High-precision Pb–Sr–Nd–Hf isotopic characterization of USGS BHVO-1 and BHVO-2 reference materials. *Geochemistry, Geophysics, Geosystems* **6**, doi:10.1029/2004GC000852.

Weis, D., Kieffer, B., Maerschalk, C. *et al.* (2006). High-precision isotopic characterization of USGS reference materials by TIMS and MC-ICP-MS. *Geochemistry, Geophysics, Geosystems* **7**, doi:10.1029/2006GC001283.

Weis, D., Kieffer, B., Hanano, D., Nobre Silva, I., Barling, J., Pretorius, W., Maerschalk, C. & Mattielli, N. (2007). Hf isotope compositions of USGS reference materials. *Geochemistry, Geophysics, Geosystems* **8**, doi:10.1029/2006GC001476.

White, W. M., Albarède, F. & Télouk, P. (2000). High-precision analysis of Pb isotope ratios by multi-collector ICP-MS. *Chemical Geology* **167**, 257–270.

Wilson, M. & Downes, H. (1992). Mafic alkaline magmatism associated with the European Cenozoic rift system. *Tectonophysics* **208**, 173–182.

Wood, D. A., Joron, J. L., Treuil, M., Norry, M. & Tarney, J. (1979). Elemental and Sr isotope variations in basic lavas from Iceland and the surrounding ocean-floor—nature of mantle source inhomogeneities. *Contributions to Mineralogy and Petrology* **70**, 319–339.